

M4 Beamline lattice

Eliana Gianfelice

**Mu2e beamline, controls and instrumentation Technical
Design Review**

6 October 2015

Contents:

- Introduction
- Beamline Geometry
- Optics
- Beam steering to target
- Off-energy optics
- Effect of quads misalignment and correction scheme
- Outlooks

Introduction

The M4 beamline is a 245 m long *new* line transporting the 8.9 GeV *proton* beam from the **Delivery Ring** to the **Mu2e** production target.



The line must contain

- an *extinction section* for removing the out-of-time particles;
- a branch, the *diagnostic line*, for accommodating the beam dump and beam diagnostics.

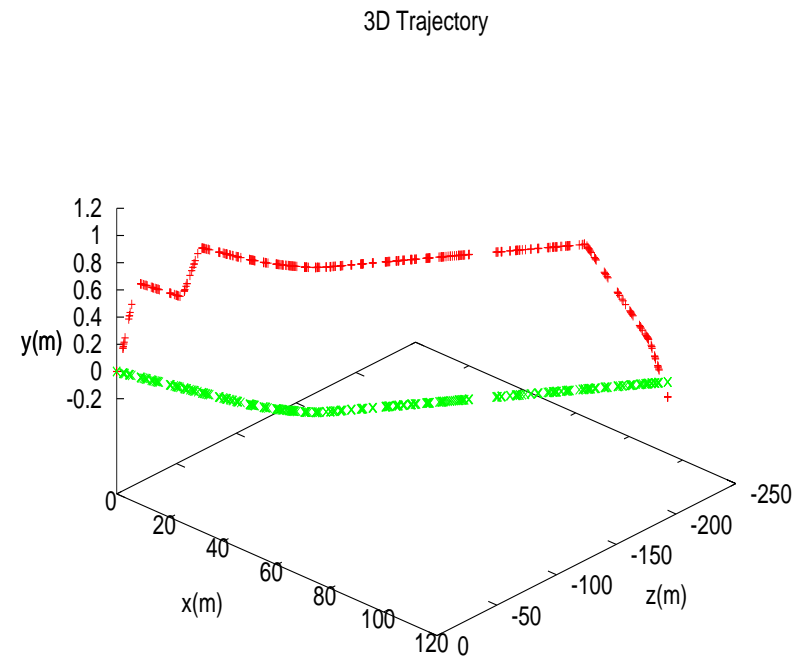
The upstream part of the line will first deliver 3.1 GeV *muon* beams to the **g-2** experiment.

The line is new, but budget constraints force us to minimize civil construction, re-use existing magnets and minimize the number of power supplies.

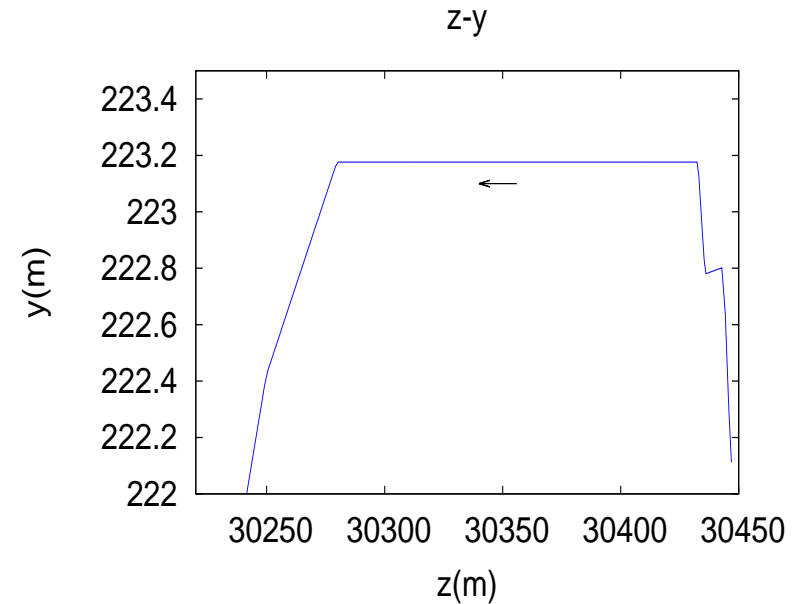
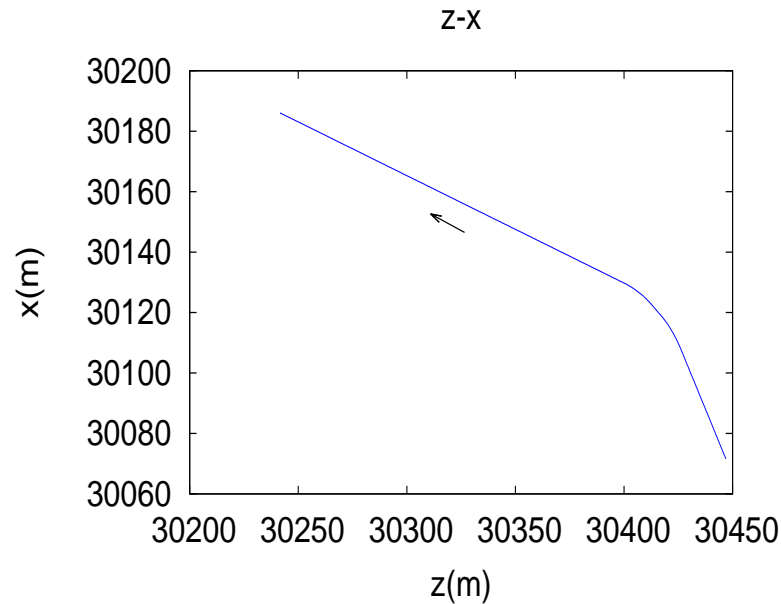
Geometry

The Muon Campus location and the M4 line layout has been chosen to avoid wetland and to minimize environmental impacts and site modifications.

- For avoiding modifications to the DR enclosure and taking advantage of existing civil construction from a previous beamline, the beam is extracted *vertically*.
- The extracted beam reaches a constant high of 1.2 m above DR level through a (almost) vertical dipole (ECMAG) and 3 vertical dipoles.
- It is steered in the horizontal plane by 6 dipoles.
- It is kicked downwards to the target by two vertical dipoles.



MADX coordinates ^a



Constraints:

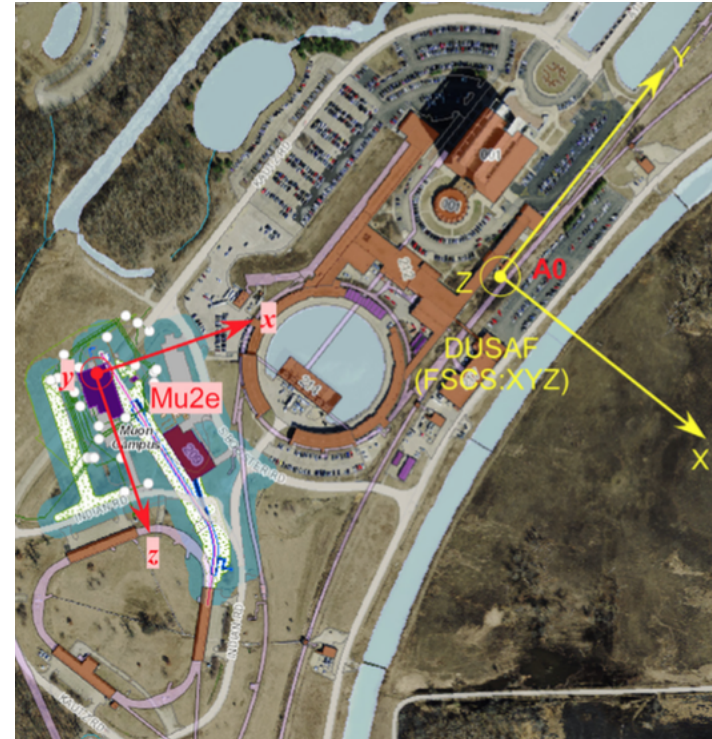
- The first three vertical dipoles strengths must be compatible with g-2 operation.
- The last two vertical dipoles are fed by the same power supply.
- The 6 horizontal dipoles depend on the same power supply and their kicks must fulfill to a fixed relationship.

^a reference point is A0

Comment

The Mu2e experiment frame is not the same as the machine one:

- The Mu2e vertical axis is collinear to the local gravity direction while MADX vertical axis is collinear with the gravity direction at A0.
- MADX does not correct for the Earth curvature.



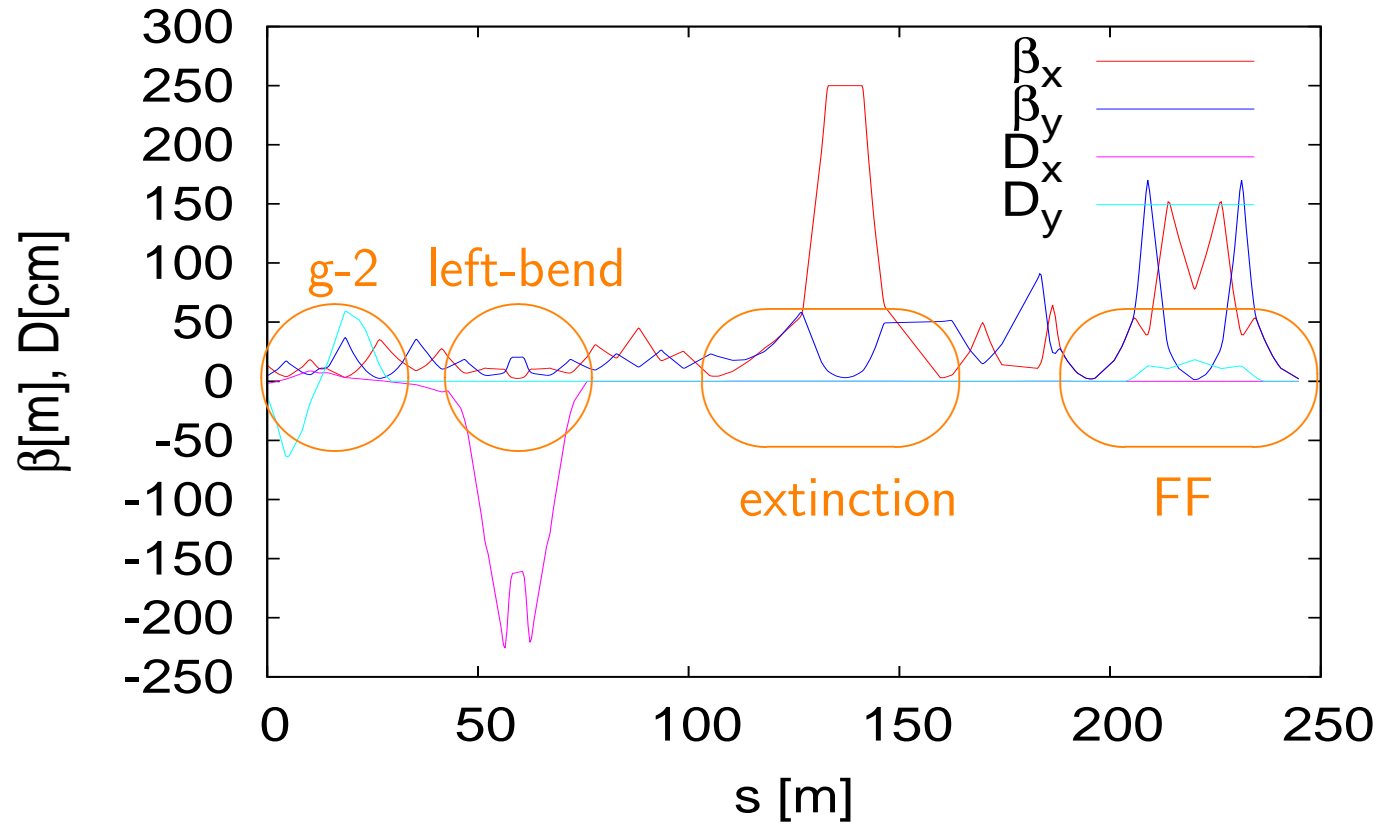
Fermi Site - MADX coordinates mapping

MADX	X	Y	Z
DUSAF	Y	Z	X

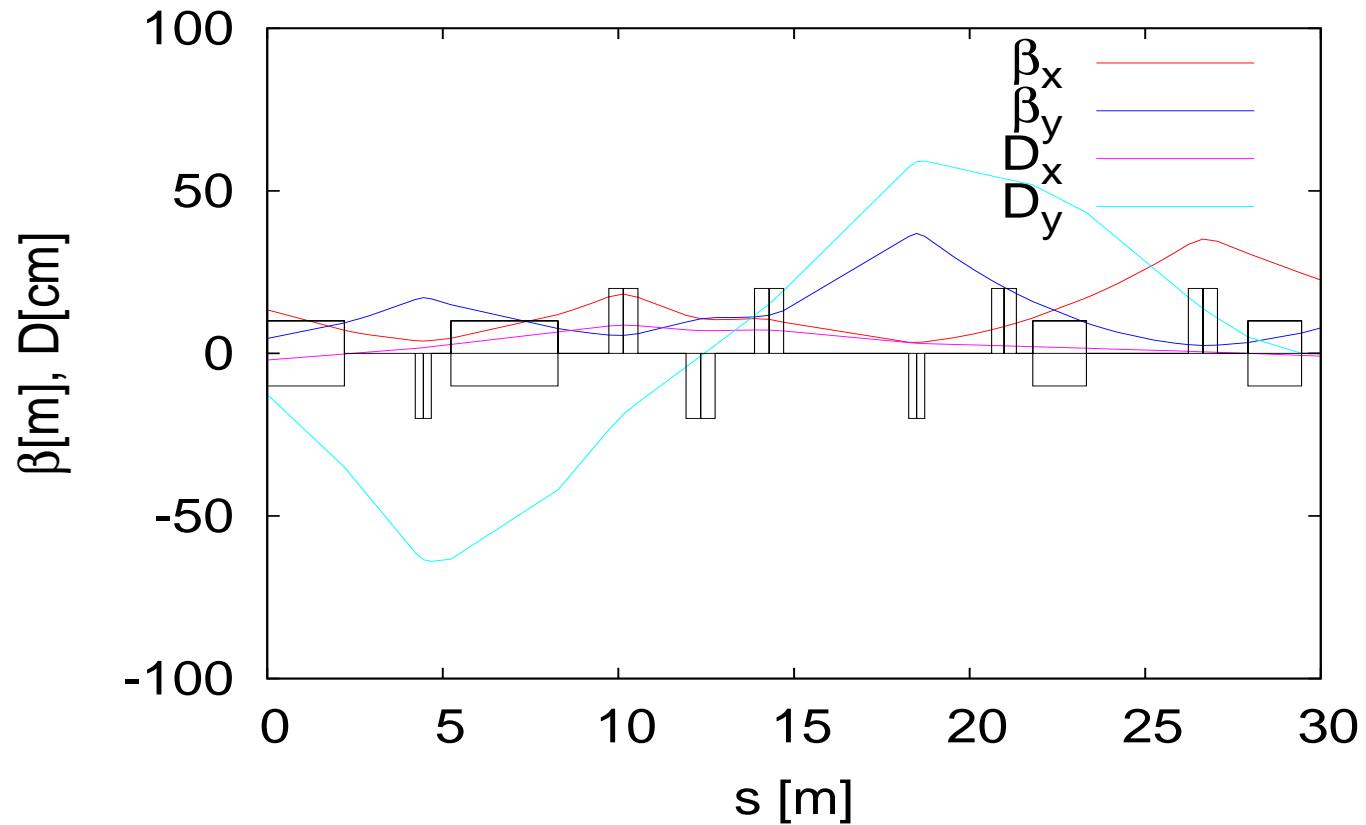
The proper transformation must be applied to the Mu2e target coordinates to get the correct target coordinates for MADX.

Optics

Overview

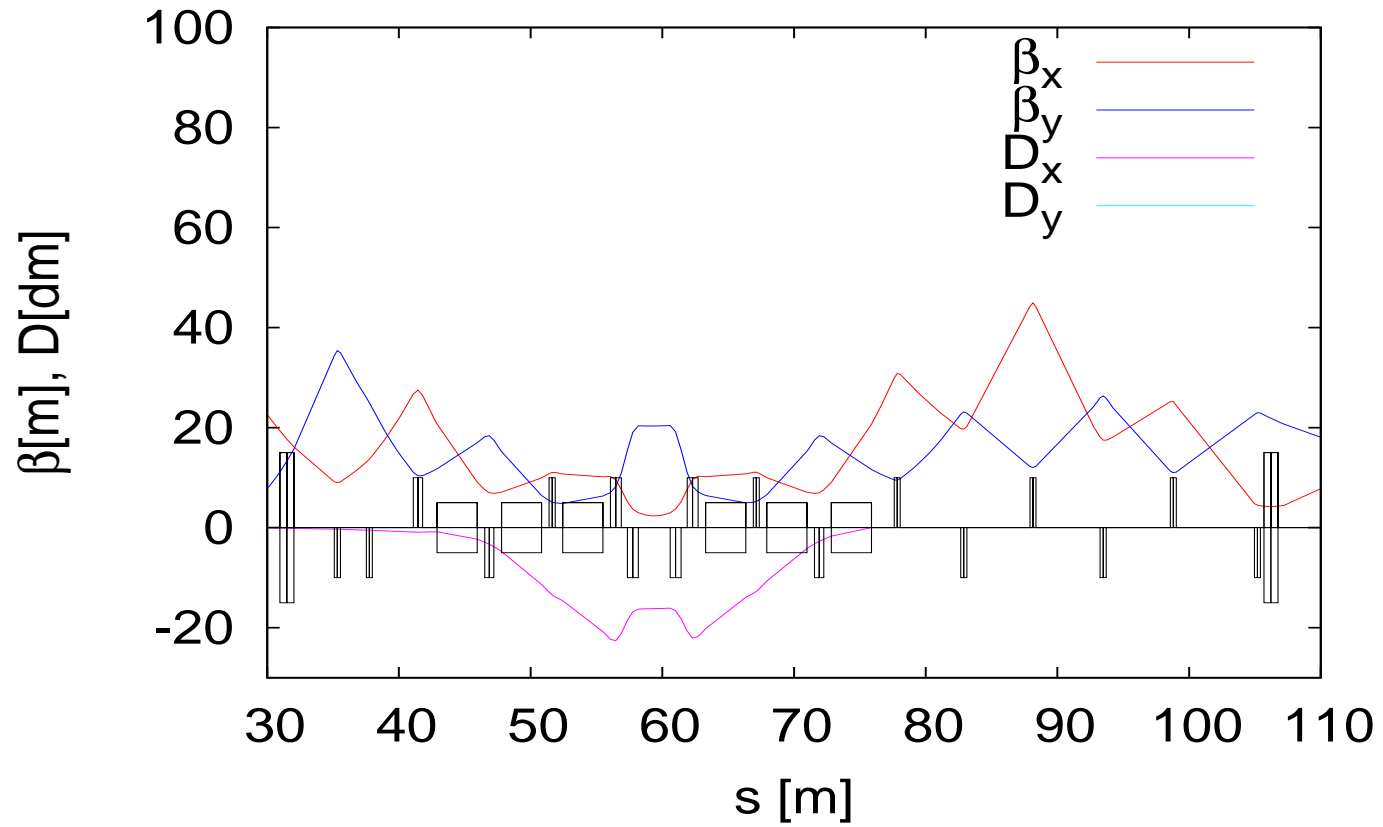


Mu2e/g-2 common part



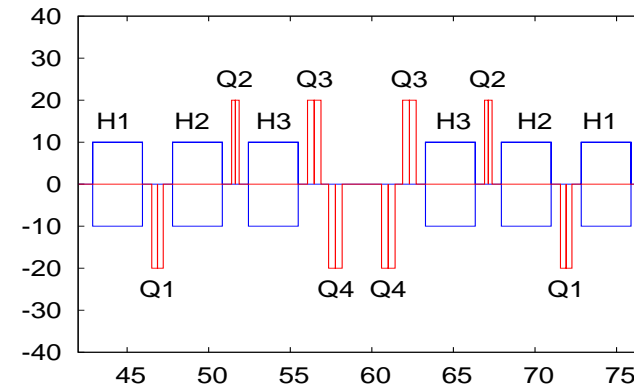
- The vertical dispersion due to the ECMAG is locally corrected.
- 7 independently powered quadrupoles.

Left bend section and matching to extinction section



Left bend section (*cont.*)

- The 6 horizontal dipoles needed to bend the beam trajectory by 41 degrees are interleaved with 8 quadrupoles powered by 4 power supplies.

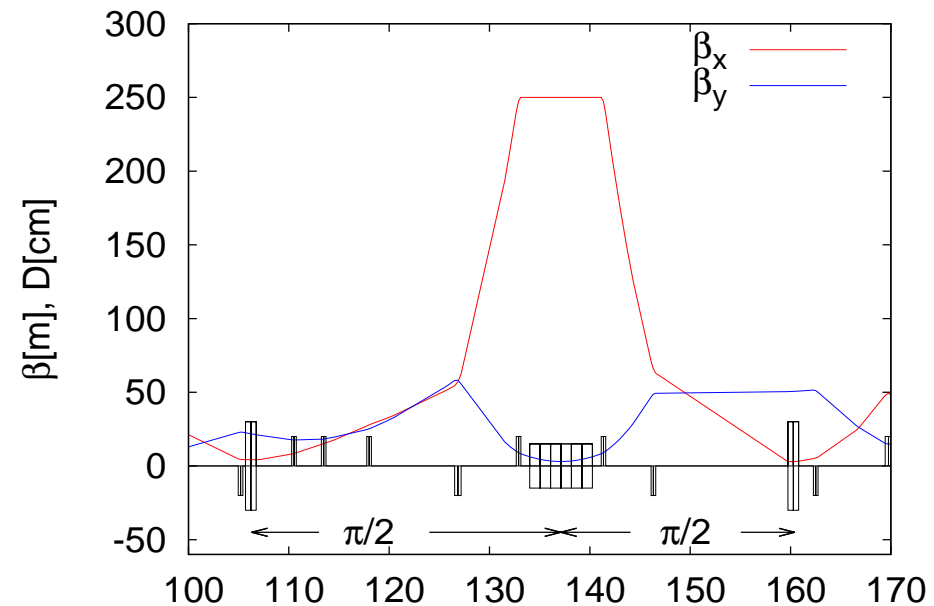


- The horizontal dispersion due to the ECMAG tilt is brought to zero.
- $\alpha_x=0$ at the first extinction section collimator is set.
- 17 quadrupoles and 9 power supplies.

Extinction section

Out-of-time to in-time particle population ratio must be kept below 10^{-10} . This is achieved by using an AC dipole. The beam is intercepted by a downstream horizontal collimator. An upstream collimator intercepts particles with small x at the AC dipole and which x' is corrected by the AC dipole so missing the downstream collimator.

- At AC dipole location:
 - Large β_x to maximize kicker effect;
 - small β_y to allow for kicker small vertical gap.
- $\Delta\mu_x = \pi/2$ between upstream collimator and kicker and between kicker and downstream collimator.
- $\alpha_x = 0$ at upstream collimator.
- Small β_x at downstream collimator.

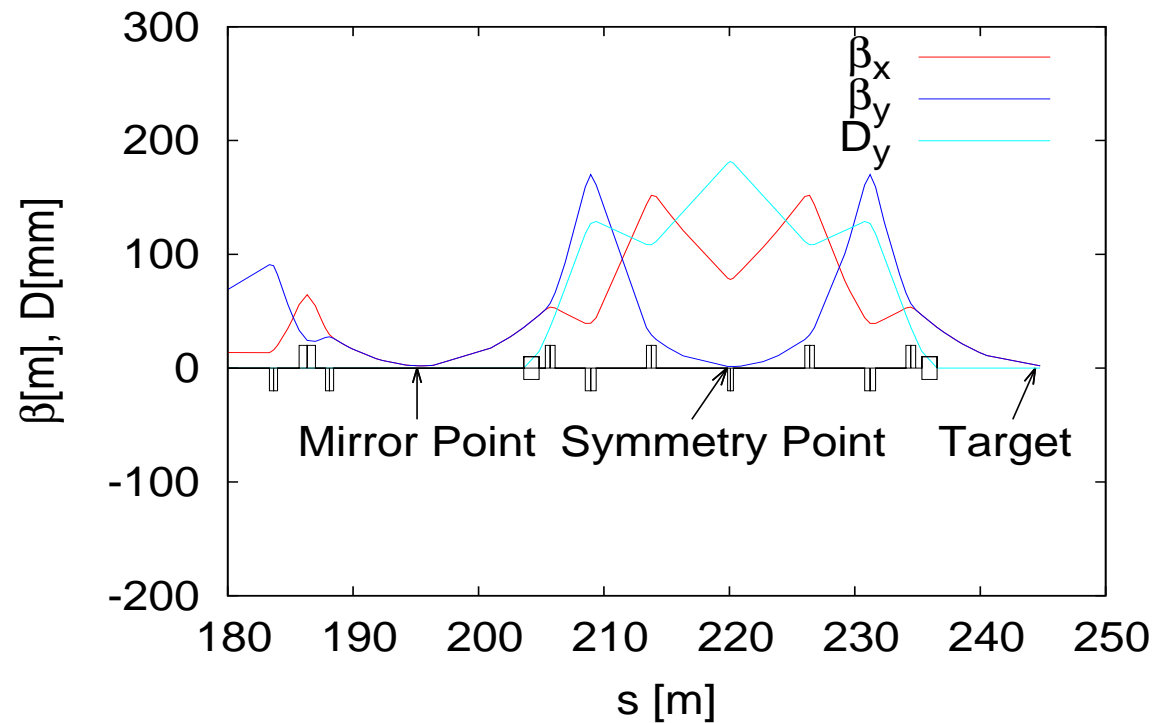


It uses 7 independently powered quads.

Final Focus section

The Final Focus section delivers the proton beam to the production target.

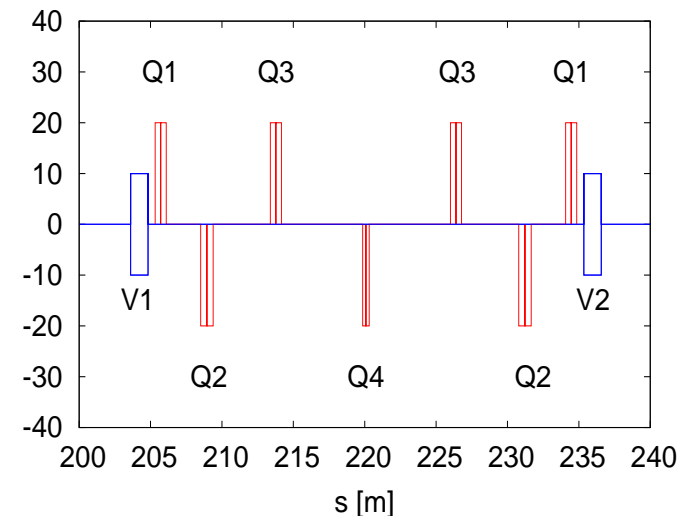
- Required beam size at the target: $2 \times 2 \text{ mm}^2$, i.e. $\beta_x^* = \beta_y^* = 2 \text{ m}$ ($\epsilon_N(95\%) = 19 \times 10^{-6} \text{ m}$).
- Two vertical dipoles ($2 \times 1.375^\circ$) bend the beam down to the target.
- The FF magnets are installed on a 1.375° vertical slope.



Final Focus section (cont.)

The particular configuration with a *Mirror Point* of the FF has been chosen for two reasons:

- Flip over β_x and β_y for y' target scans by inverting the polarity of the 7 FF quadrupoles with no need for re-matching.
- Under the assumption of no errors in the downstream part, diagnostics at the mirror point will deliver direct informations of the beam parameters at the inaccessible target.



Final Focus section (*cont.*)

The FF *Mirror Point* is obtained by asking

$$T(MP \rightarrow FF) = \begin{pmatrix} \pm \mathcal{I} & \underline{0} \\ \underline{0} & \pm \mathcal{I} \end{pmatrix}$$

- The $\pm \mathcal{I}$ transformation is only approximatively obtained:

With $\beta_1 = \beta_2 \equiv \beta$ and $\alpha_1 = \alpha_2 = 0$

$$T(MP \rightarrow FF) = \begin{pmatrix} \cos \Delta\mu & \beta \sin \Delta\mu \\ -\sin \Delta\mu / \beta & \cos \Delta\mu \end{pmatrix} \quad \Delta\mu \equiv \mu_{FF} - \mu_{MP}$$

which is a $\pm \mathcal{I}$ transformation if in addition $\Delta\mu = n\pi$.

Owing to the symmetry the conditions are

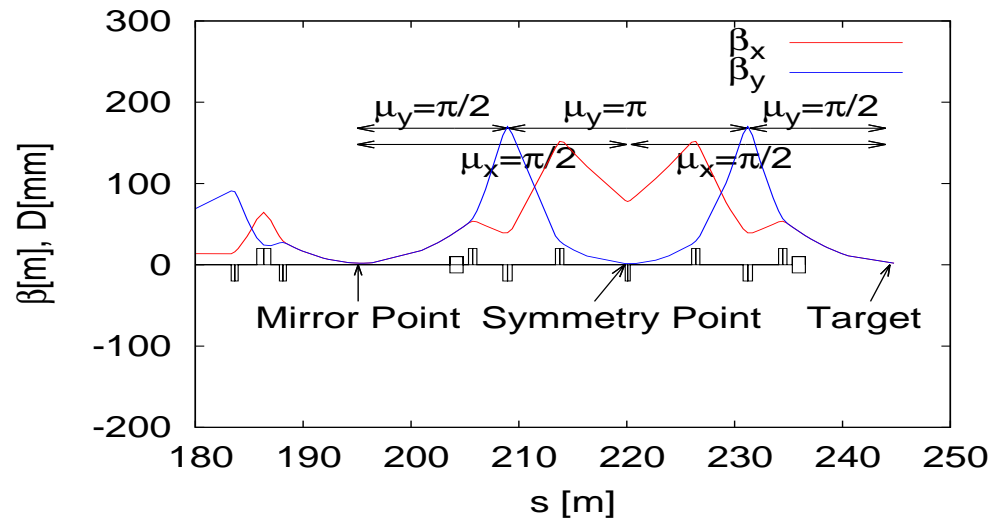
$$\alpha_{x,SP} = \alpha_{y,SP} = 0 \quad D'_{y,SP} = 0$$

$$\Delta\mu_x = n\pi \quad \Delta\mu_y = m\pi$$

which cannot be satisfied with only 4 free parameters.

Final Focus section (cont.)

However it turns out that $\Delta\mu \simeq 2\pi$ (or π) because of the β minima:



In our case it is $\Delta\mu_y/2\pi \simeq 0.925$ and $\Delta\mu_x/2\pi \simeq 0.496$.

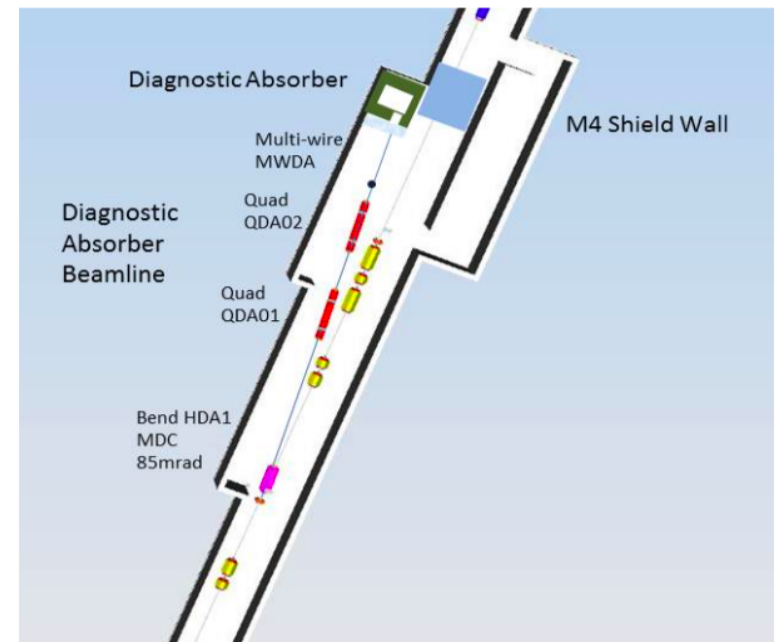
Including matching sections and g-2 common part, the M4 line uses

- 43 quadrupoles
- 33 power supplies

Diagnostic line

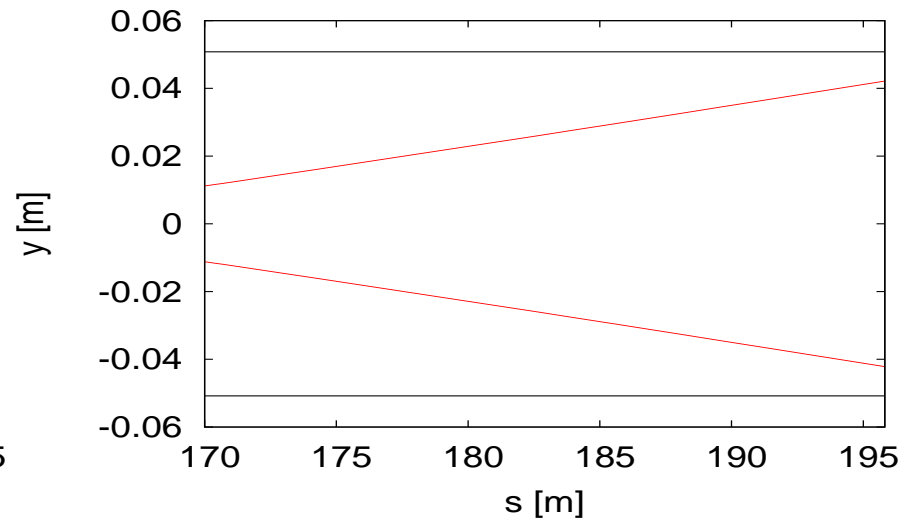
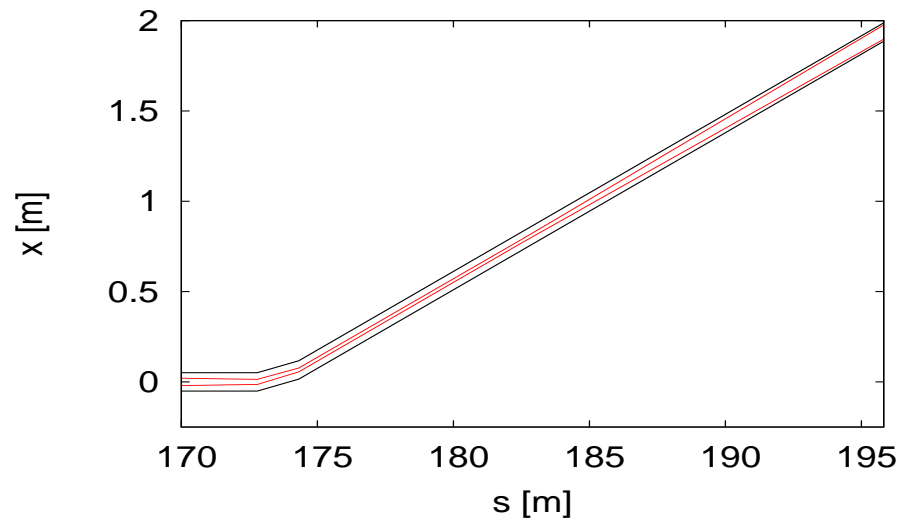
The line has a branch behind the extinction section containing a beam dump and a MW for commissioning, tuning, and beam studies.

- A dipole at 174 m kicks the beam horizontally by 87 mrad.
- The beam is dumped at 195 m on a steel absorber embedded into concrete blocks.
- A MW monitor measures the beam profile.
- Two spare quadrupoles introduced for diagnostic purposes.



Diagnostic line (cont.)

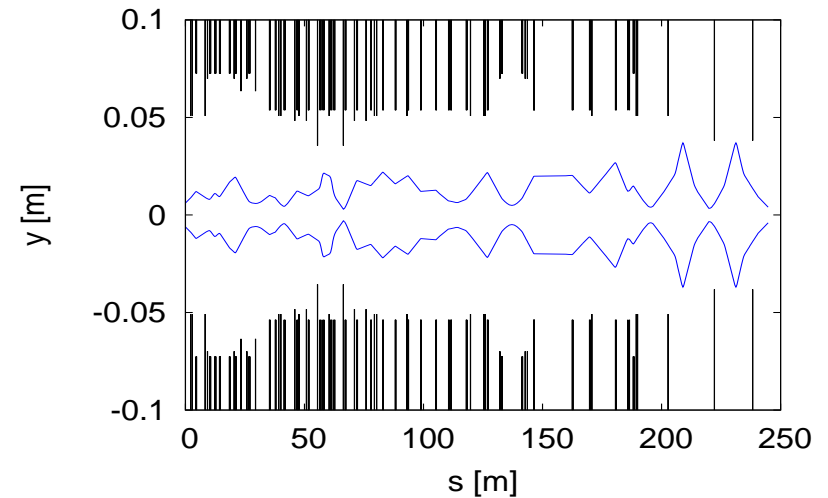
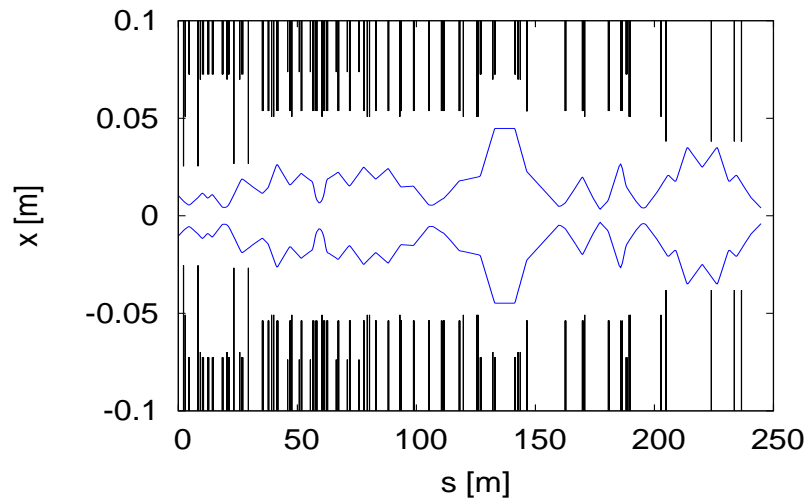
Beam envelopes (5σ) in the diagnostic line.



Beam dimension at dump: $17.2 \times 17.8 \text{ mm}^2$

M4 Beam line aperture

$\pm 5\sigma$ envelopes with $\epsilon_x^N = \epsilon_y^N$ (95%) = 19×10^{-6} m and $\Delta p/p$ (95%) = $\pm 0.5\%$



$\check{n}_x = 6.1$ at 216 m (VT940) (*)

$\check{n}_y = 10$ at 183 m (Q934) (*)

(*) it includes the energy spread contribution

M4 Beam line aperture (*cont.*)

Considering

- 20% β -beating and 10% dispersion beating, k
- maximum orbit excursion $\hat{z}_{co} = 4.5$ mm
- energy offset $\delta = 1\%$

$$n_z = \left[r_z - \hat{z}_{co} \left(\frac{\beta_z}{\hat{\beta}_z} \right)^{1/2} - k |D_z \delta| \right] / k \sigma_z$$

The minimum number of σ are reduced to $\check{n}_x = 5.1$ and $\check{n}_y = 8.5$

Beam scans at target

It is crucial that the beam hits the target correctly which is *fixed* inside the production solenoid.

Experimenters have asked for the possibility of orthogonal scans of beam position by ± 1 cm and beam angle by $\pm 0.8^\circ$.

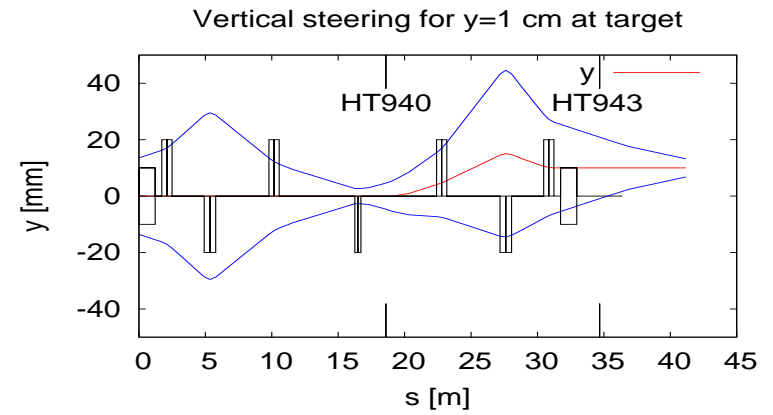
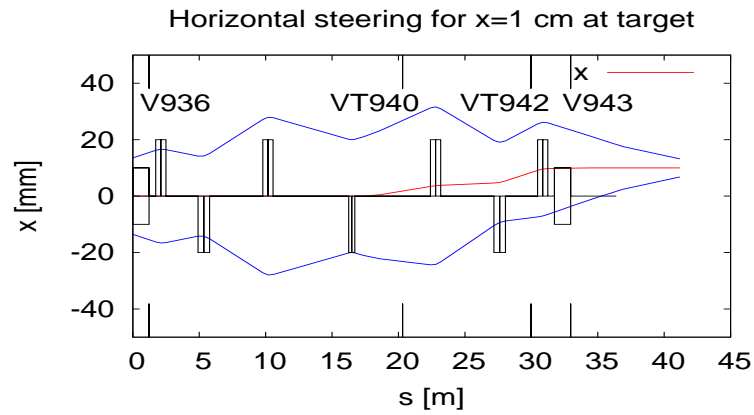
For this purpose we use the last 2 horizontal and vertical correctors.

Apertures

	type	d_x cm (")	d_y cm (")
Q941	LQC	30.48 (12)	30.48 (12)
Q942	LQD	30.48 (12)	30.48 (12)
Q943	LQC	30.48 (12)	30.48 (12)
HT940	CDA	25.4 (10)	7.62 (3)
HT943	CDA	25.4 (10)	7.62 (3)
VT940	CDA	7.62 (3)	25.4 (10)
VT943	CDA	7.62 (3)	25.4 (10)
V943	CDA	7.62 (3)	25.4 (10)

CDA's apertures in the bend plane could be stretched to 12".

Beam position scan - $\pm 4\sigma$ envelope

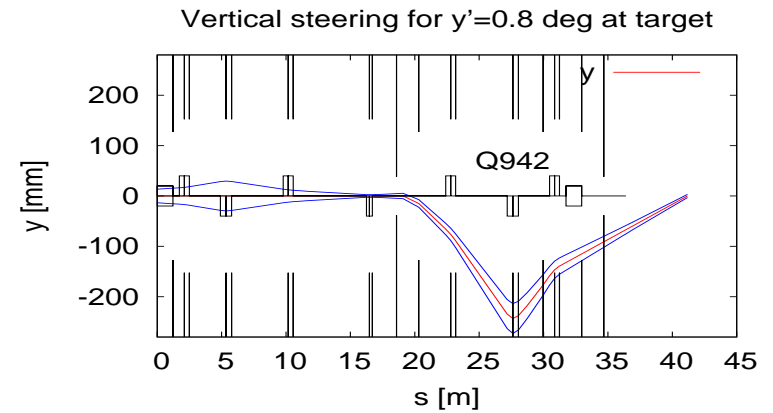
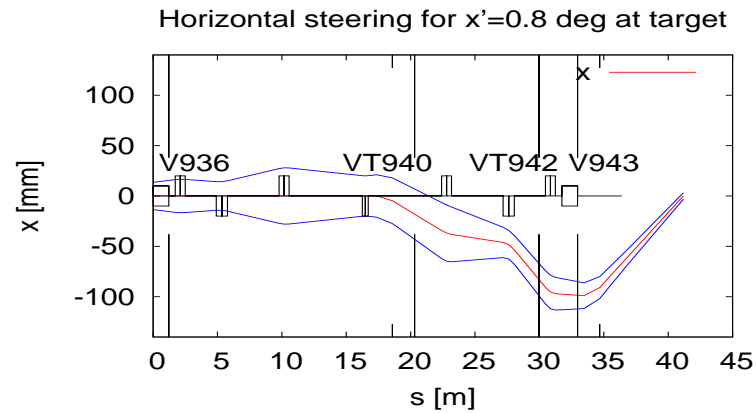


kicks (mrad)

HT940	HT943
0.78	-0.09

VT940	VT942
1.50	0.28

Beam angle scan - $\pm 4\sigma$ envelope



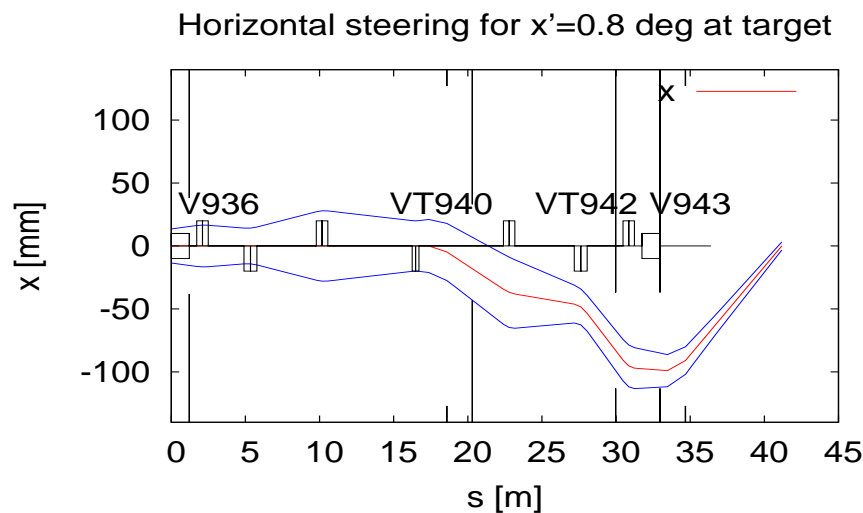
kicks (mrad)

HT940	HT943
-7.75	14.87

VT940	VT942
-24.3	6.8

Beam angle scan (cont.)

The 0.8° horizontal angle scan is limited by the last 3 vertical dipole width. For this reason they will be mounted on supports moveable horizontally by ± 7.6 cm ($\pm 2.99''$) which allows a full scan:



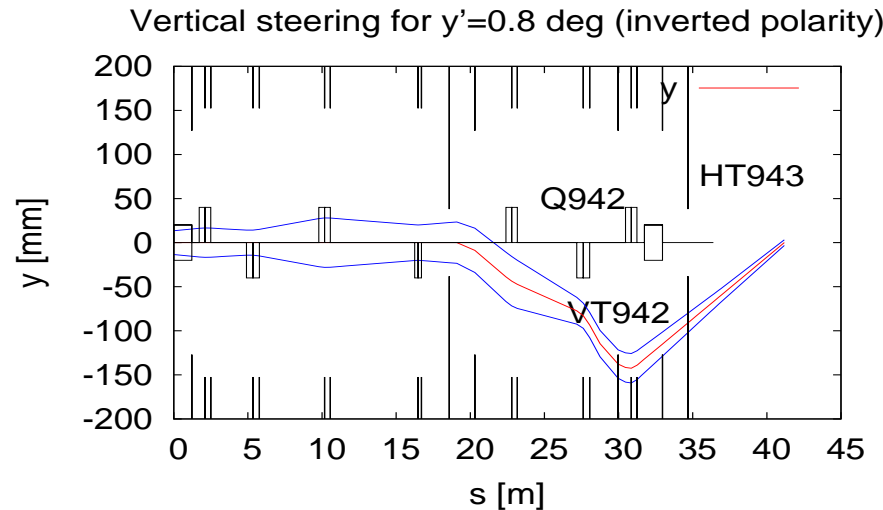
dipoles horizontal shift (cm)

VT940	VT942	V943
0.3	6.0	7.4

Beam angle scan (cont.)

The vertical angle scan is limited by the vertical aperture at the quadrupoles Q942 and Q943 in addition to the dipoles VT942 and HT943.

The situation is improved by *flipping* the FF quads polarity:

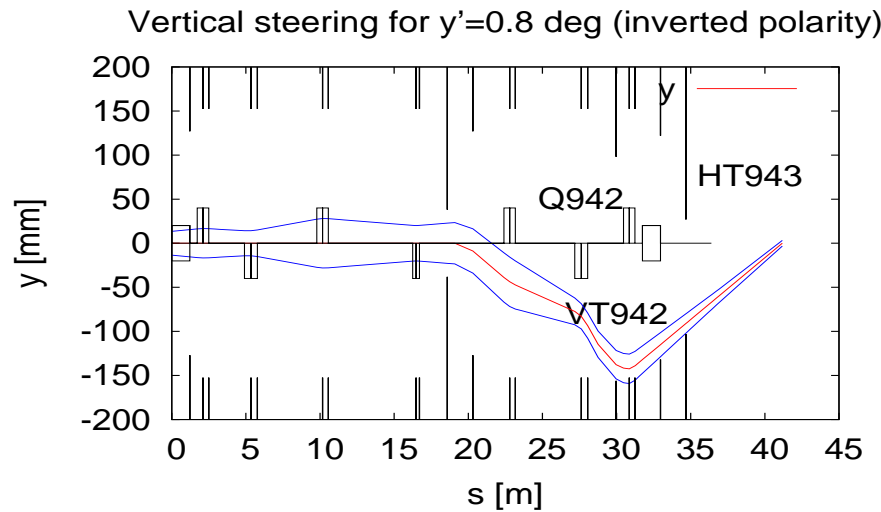


kicks (mrad)

VT940	VT942
-14.3	22.8

- It is still needed to move 3 dipoles.
- Tight at Q943, however scans will be performed at low intensity!

Beam angle scan (cont.)



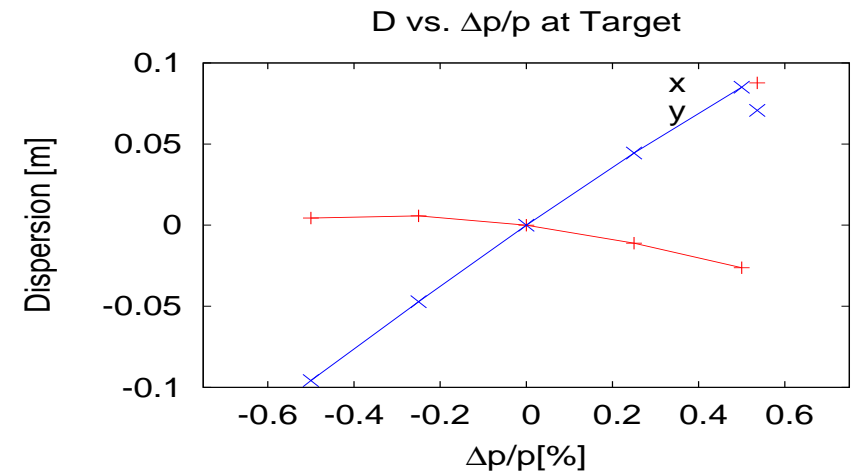
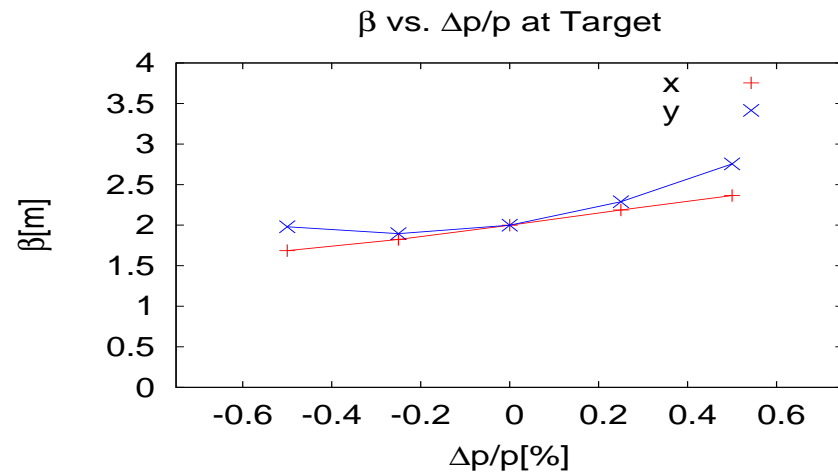
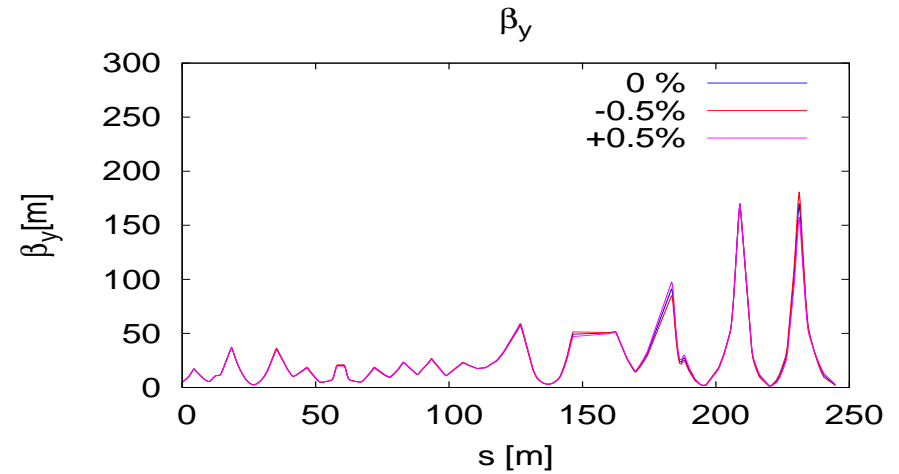
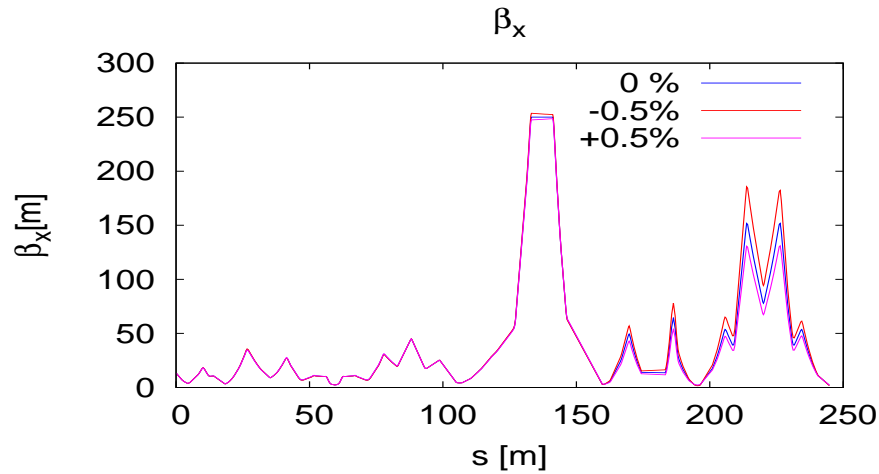
dipoles vertical shift (cm)

VT942	V943	HT943
2.7	0.5	6.4

- Field quality will forbid such a large beam offset at the quadrupole: angle scans up to 0.4° are more realistic.
- Polarity flip is for diagnostic purpose: if large angles are required for hitting the target correctly, the line will be re-aligned.

Off-energy optics

Maximum particle $\Delta p/p$ is expected to be $\pm 0.3\%$.



Off-energy optics (*cont.*)

Twiss (m), and dispersion (m) at Target

	β_x	β_y	D_x	D_y
-0.5%	1.7	2.0	0.004	-0.096
0. %	2	2	0	0
0.5%	2.4	2.8	-0.026	0.085

Twiss parameters at extinction section devices:

$\Delta p/p = -0.5\%$

	β_x	$\Delta\mu_x$
	(m)	(deg)
MCOL924	4.2	0.0
AC	253.0	89.9
MCOL931	3.0	98.9

$\Delta p/p = 0\%$

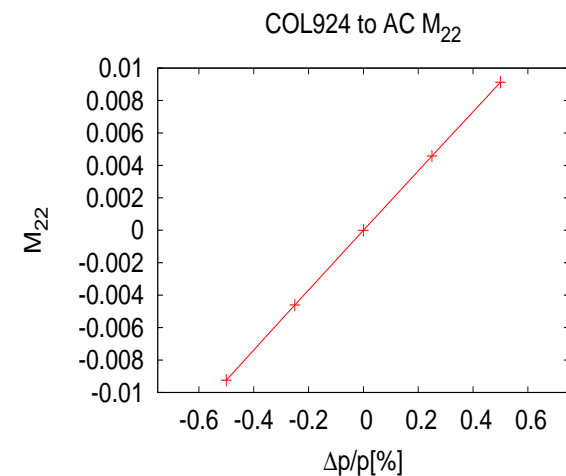
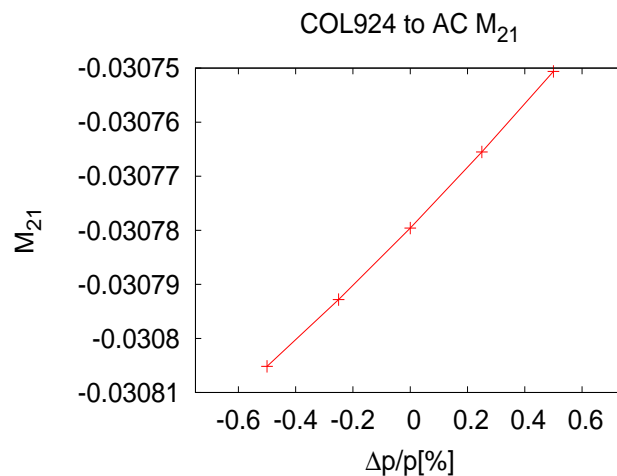
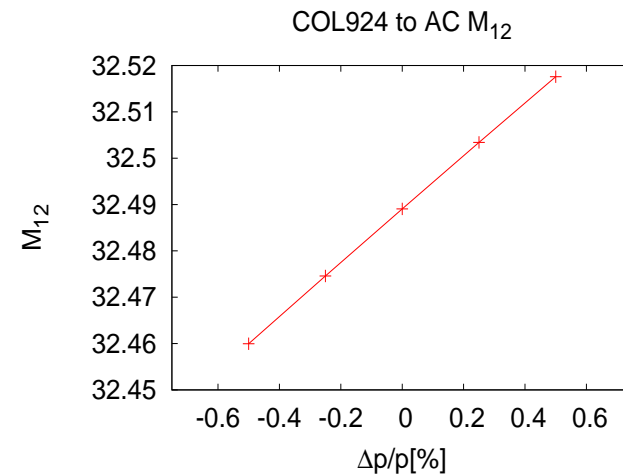
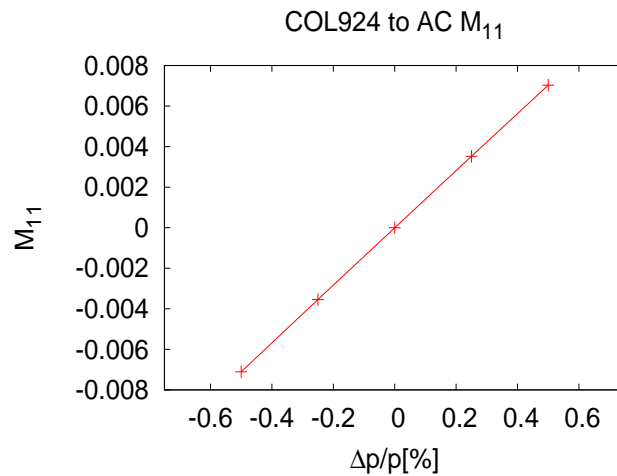
	β_x	$\Delta\mu_x$
	(m)	(deg)
COL924	4.2	0
AC	250.0	90
COL931	3.0	90

$\Delta p/p = +0.5\%$

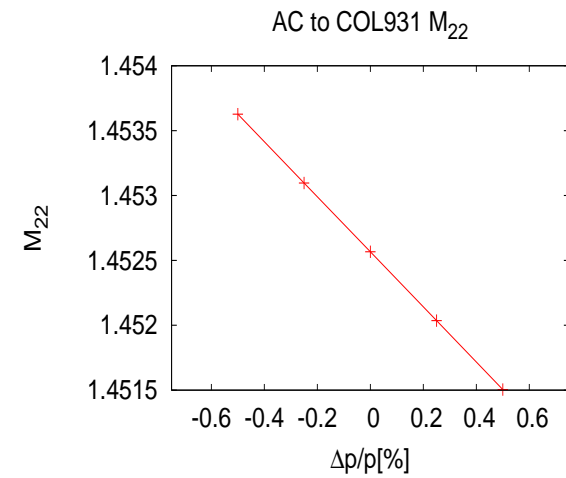
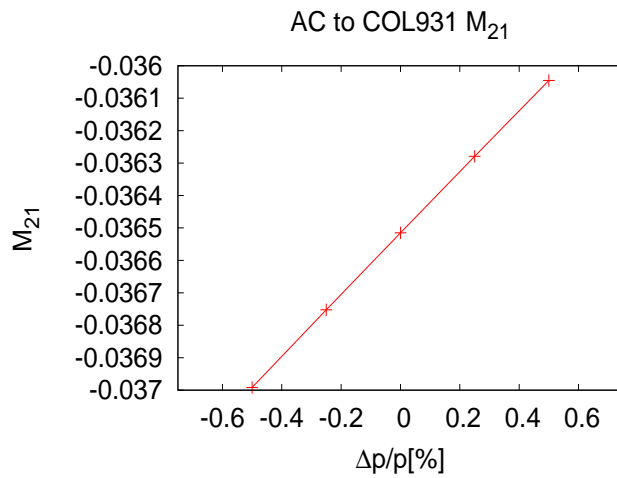
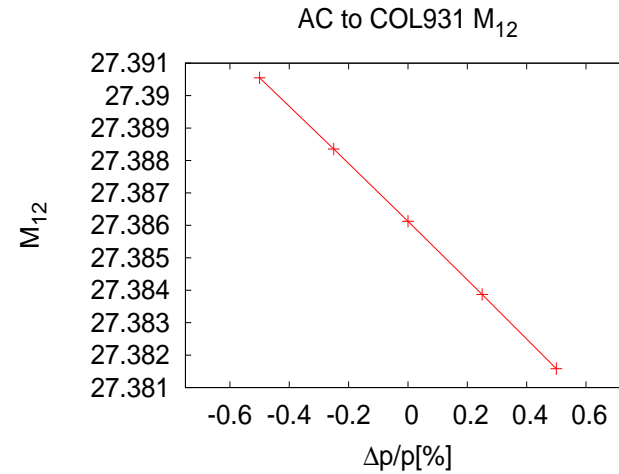
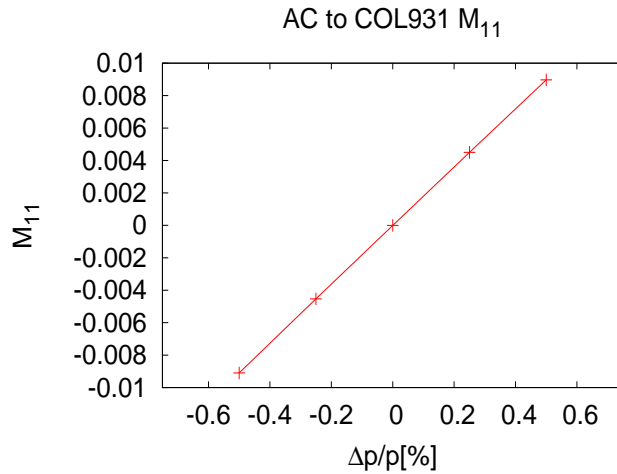
	β_x	$\Delta\mu_x$
	(m)	(deg)
MCOL924	4.3	0.0
AC	248.0	90.1
MCOL931	3.1	81.3

Off-energy optics (*cont.*)

However what really matters are the elements of the horizontal transport matrix between the extinction section elements!



Off-energy optics (cont.)



Simulations with *realistic* 6D beam distribution show that the out-of-time to in-time particle population ratio is reduced from 10^{-5} to 10^{-12} .

Alignment errors and trajectory distortion correction

Guidelines:

- Place monitors and correctors where β is large.
- Phase advance between adjacent monitors should be not too much larger than 90^0 .
- There should be always a monitor between adjacent correctors for avoiding unseen bumps.
- Upstream each monitor there should be a corrector at $\sim 90^0$ phase advance.

However owing to the peculiarity of this line, the optics has *no* regularity and it is not simple to find optimal locations for monitors and correctors.

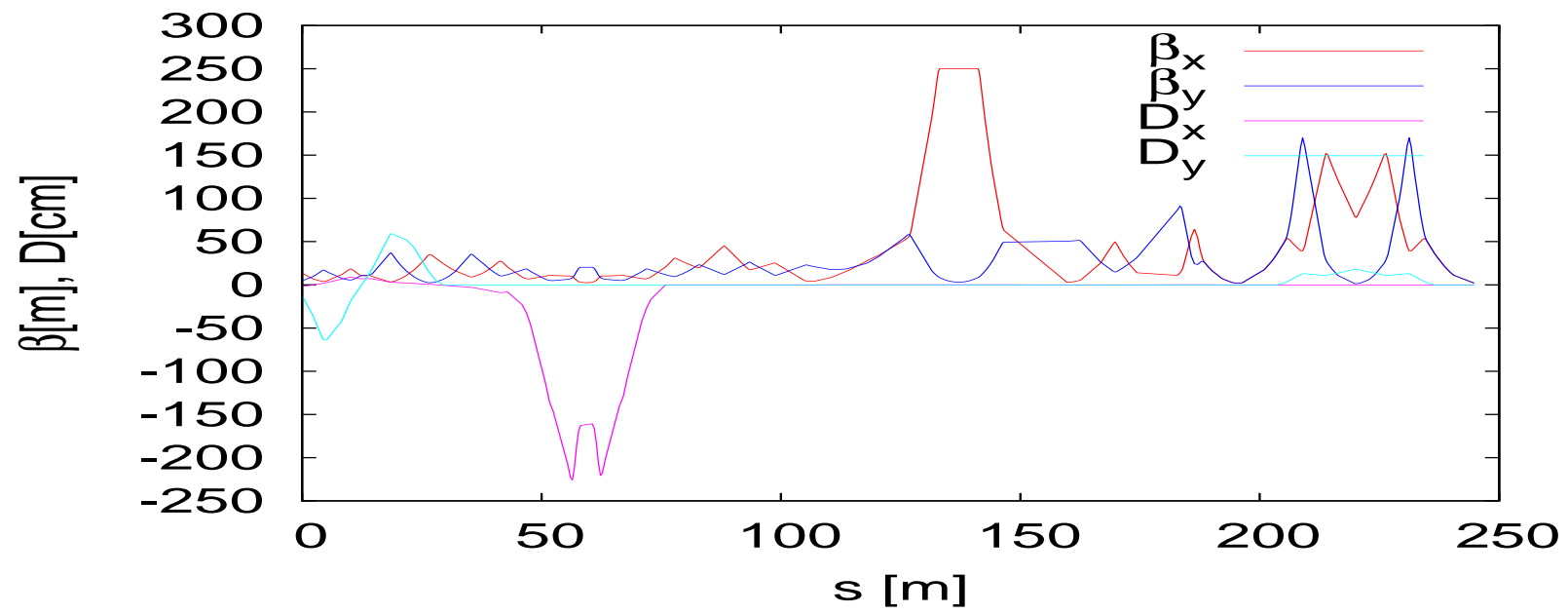
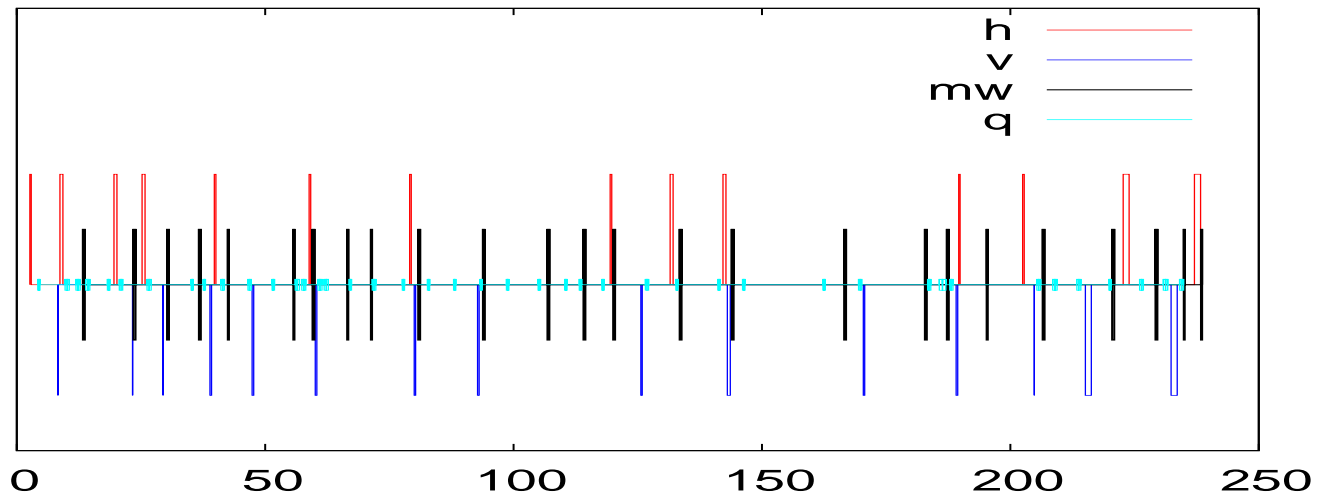
Inserted:

- 25 monitors
- 11 VTs + 4 “fake kickers” for V901, V906, V907 and V936
- 14 HTs

The position of monitors and correctors was refined through “multi-seeds” simulations. A Proportional Wire Chamber at the line entry will be used for extraction troubleshooting.

The other M4 monitors are Multiwire chambers allowing measuring beam position and profiles in both horizontal and vertical planes.

Two MW monitors at the exit separated by a 3.5 m drift space allow for monitoring the beam delivery to target.



β and phase advance difference at horizontal correctors and MW

	s	β_x	$\Delta\mu_x$		s	β_x	$\Delta\mu_x$		s	β_x	$\Delta\mu_x$
	m	m	deg		m	m	deg		m	m	deg
HT900	3.	6.	0.	HT901	9.	16.	59.	MW903Nu	14.	11.	19.
HT905	20.	6.	69.	MW906Nu	24.	20.	20.	HT906	26.	31.	4.
MW907Nu	31.	20.	10.	MW908Nu	37.	12.	30.	HT909	40.	22.	11.
MW910Tx	43.	22.	6.	MW912Tx	56.	10.	77.	MW914Nu	60.	2.	63.
HT915	62.	8.	31.	MW916Tx	67.	11.	27.	MW917Tx	72.	7.	32.
HT919	79.	27.	30.	MW919Nu	81.	23.	4.	MW922Nu	94.	18.	28.
MW924Nu	107.	4.	76.	MW926Nu	114.	18.	51.	HT927	120.	32.	13.
MW927Nu	120.	34.	1.	HT928	132.	217.	11.	MW929Nu	134.	250.	0.
HT930	143.	187.	2.	MW930Nu	144.	126.	1.	MW932Nu	167.	27.	143.
MW933Nu	183.	13.	153.	MW935Nu	188.	39.	8.	HT936A	190.	17.	5.
MW936Tx	195.	2.	72.	HT936B	203.	29.	73.	MW937Nu	207.	48.	6.
MW940Nu	221.	85.	10.	HT940	224.	122.	2.	MW941Nu	230.	68.	3.
MW943aTx	235.	49.	7.	HT943	238.	23.	5.	MW943bTx	239.	21.	1.

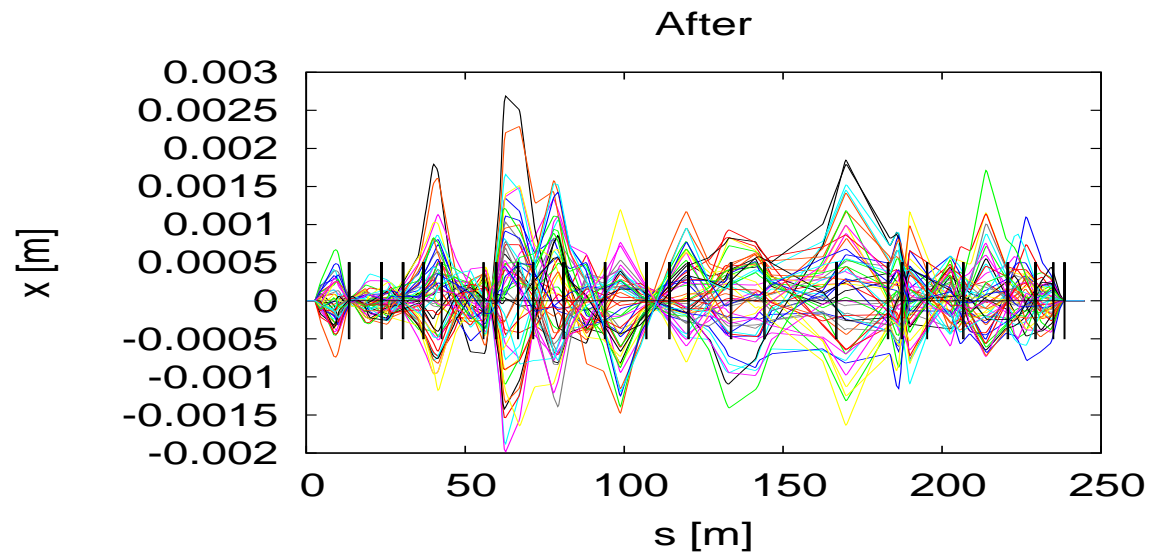
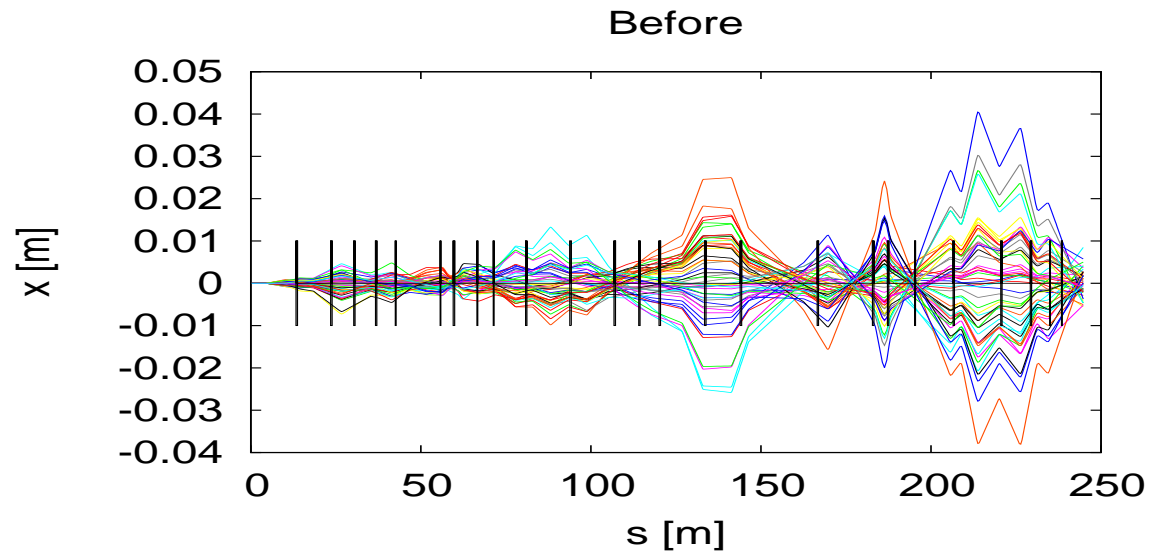
β and phase advance difference at vertical correctors and MW

	s	β_y	$\Delta\mu_y$		s	β_y	$\Delta\mu_y$		s	β_y	$\Delta\mu_y$
	m	m	deg		m	m	deg		m	m	deg
V901K	8.	8.	49.	MW903Nu	14.	11.	41.	V906K	23.	9.	30.
MW906Nu	24.	7.	4.	V907K	29.	6.	87.	MW907Nu	31.	10.	9.
MW908Nu	37.	28.	17.	VT909	39.	18.	5.	MW910Tx	43.	12.	16.
VT911	48.	16.	19.	MW912Tx	56.	7.	73.	MW914Nu	60.	20.	17.
VT914	60.	20.	1.	MW916Tx	67.	5.	53.	MW917Tx	72.	17.	32.
VT919	80.	15.	40.	MW919Nu	81.	18.	3.	VT921	93.	25.	40.
MW922Nu	94.	24.	3.	MW924Nu	107.	21.	46.	MW926Nu	114.	20.	22.
MW927Nu	120.	33.	14.	VT927	126.	55.	7.	MW929Nu	134.	7.	23.
VT930	144.	23.	111.	MW930Nu	144.	29.	2.	MW932Nu	167.	26.	29.
VT933	171.	17.	12.	MW933Nu	183.	90.	19.	MW935Nu	188.	26.	7.
VT936	189.	20.	4.	MW936Tx	195.	2.	73.	V936K	205.	47.	77.
MW937Nu	207.	93.	2.	VT940	216.	11.	13.	MW940Nu	221.	2.	105.
MW941Nu	230.	114.	55.	VT942	234.	82.	2.	MW943aTx	235.	49.	1.
MW943bTx	239.	21.	6.								

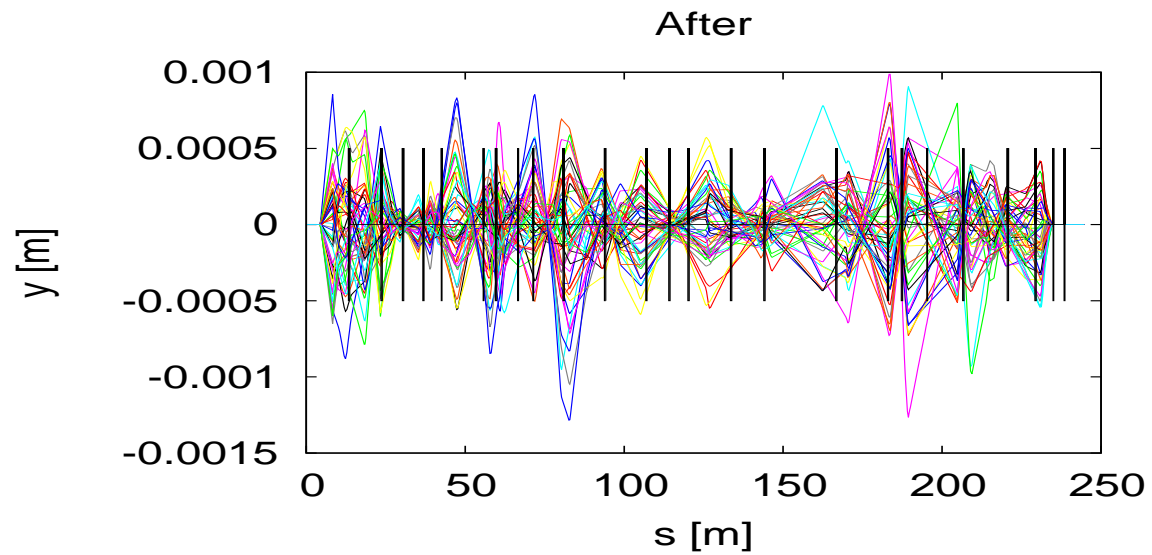
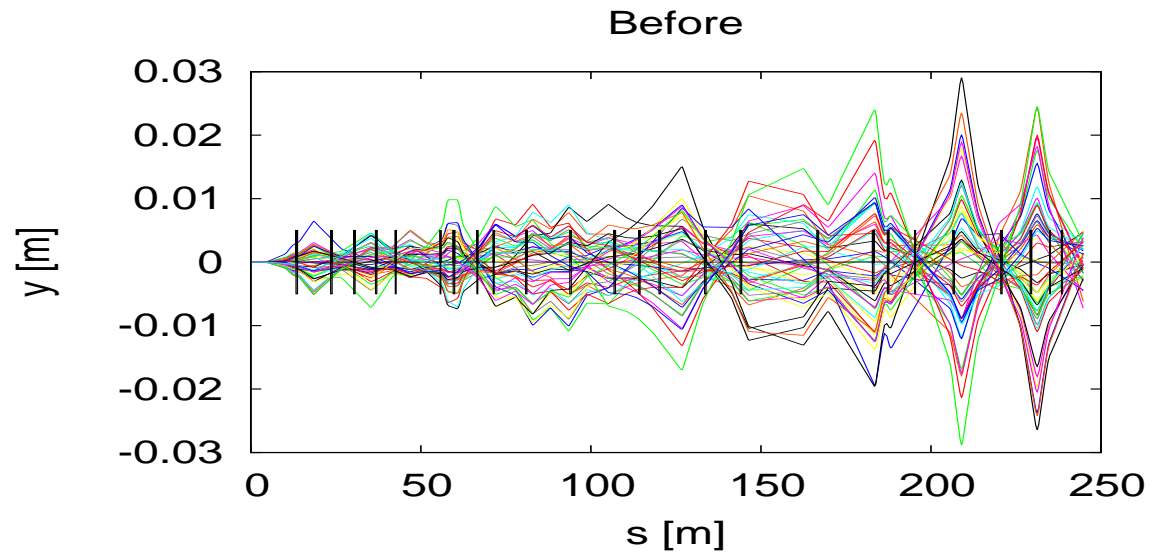
Trajectory studies done with MADX

- Quadrupole misalignment: $\delta x_{rms}^Q = \delta y_{rms}^Q = 500 \mu\text{m}$
- no starting trajectory errors
- SVD algorithm
- 50 seeds quad misalignment error
- monitors:
 - no monitor errors
 - 10% calibration errors
 - 500 μm rms misalignment
 - 80% availability
 - 10% calibration errors + 500 μm rms misalignment + 80% availability
- last 2 horizontal and vertical correctors used for “empirical” steering at the target

Horizontal:



Vertical:



Before correction (mm)(*)

x_{rms}	\hat{x}	y_{rms}	\hat{y}
4.854 ± 2.392	15.193 ± 8.323	3.877 ± 1.687	12.593 ± 6.303

After correction (mm)(*)

x_{rms}	\hat{x}	y_{rms}	\hat{y}
0.387 ± 0.129	1.246 ± 0.441	0.198 ± 0.056	0.689 ± 0.222

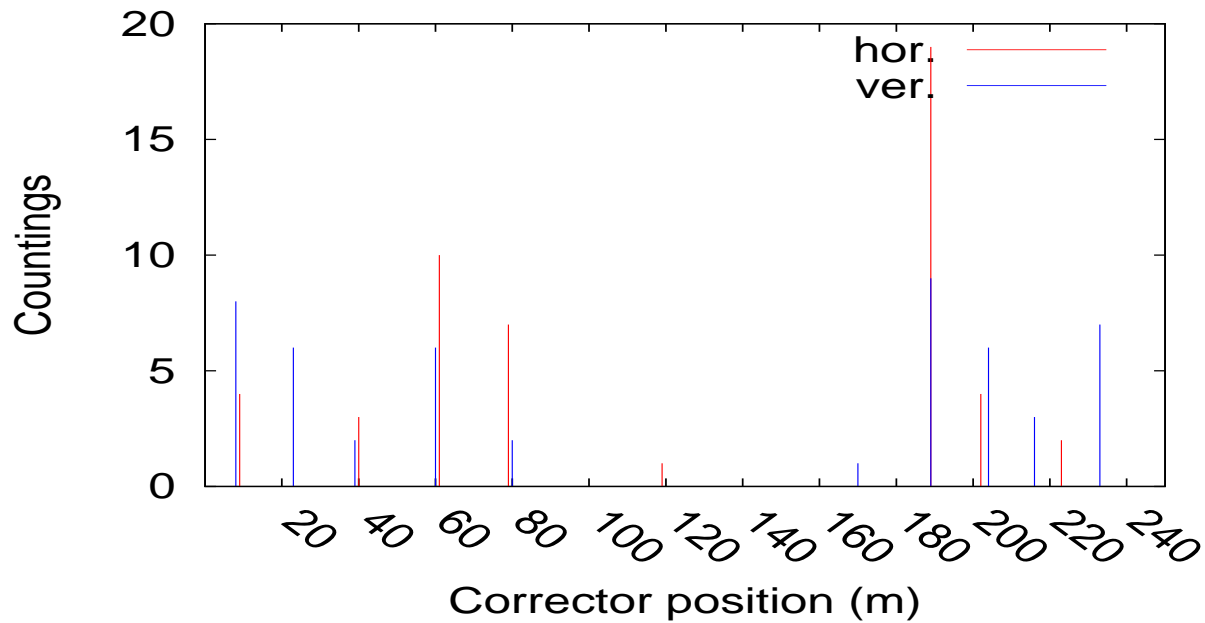
(*) Averages over 50 seeds

Maximum correction kick (mrad)(*)

$\langle \hat{\theta}_x \rangle$	$\langle \hat{\theta}_y \rangle$
0.273 ± 0.137	0.279 ± 0.088

(*) Averages over 50 seeds

Maximum kick distribution

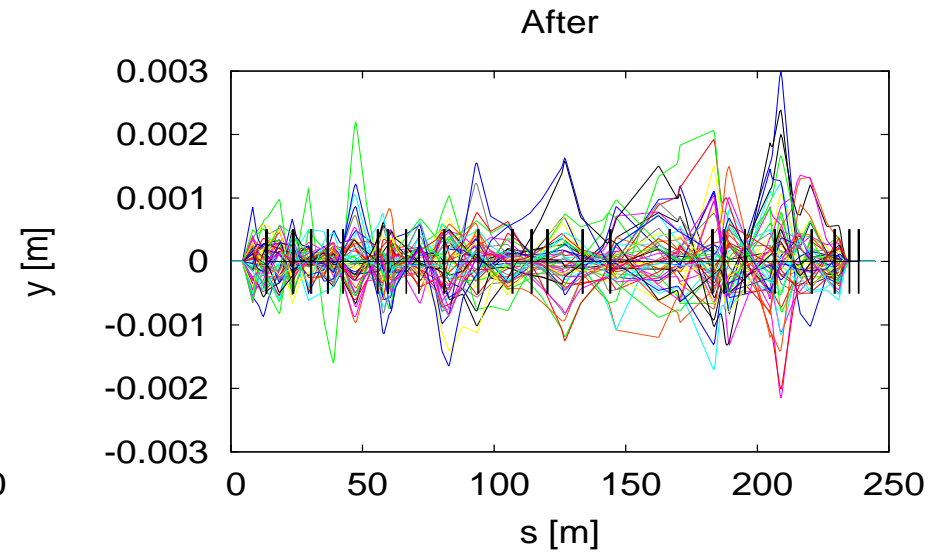
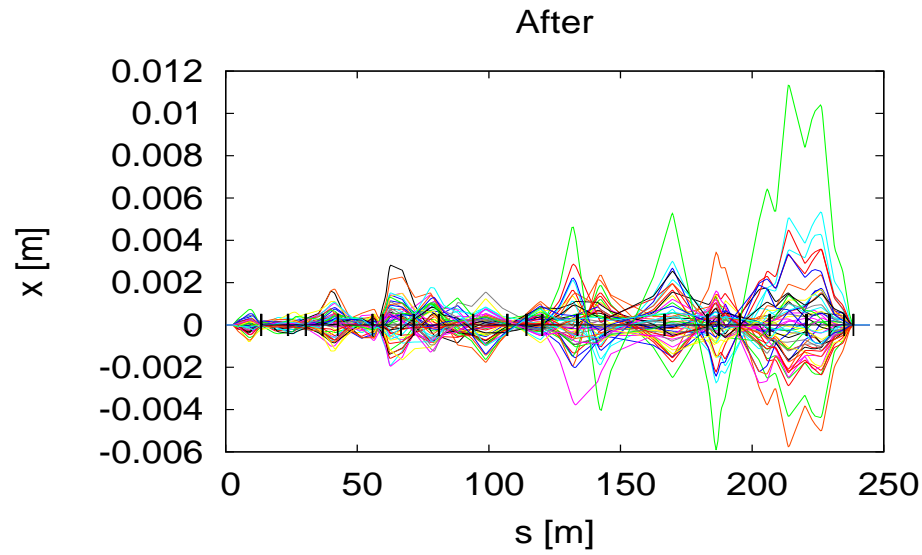


Correction kicks (SVD+steering) (mrad)

HT940	0.076 ± 0.004
HT943	0.054 ± 0.001
VT940	0.087 ± 0.020
VT942	0.104 ± 0.011

Effect of monitors errors

10% monitor calibration error (50 seeds)



10% monitor calibration error (*cont.*)

After correction (mm)(*)

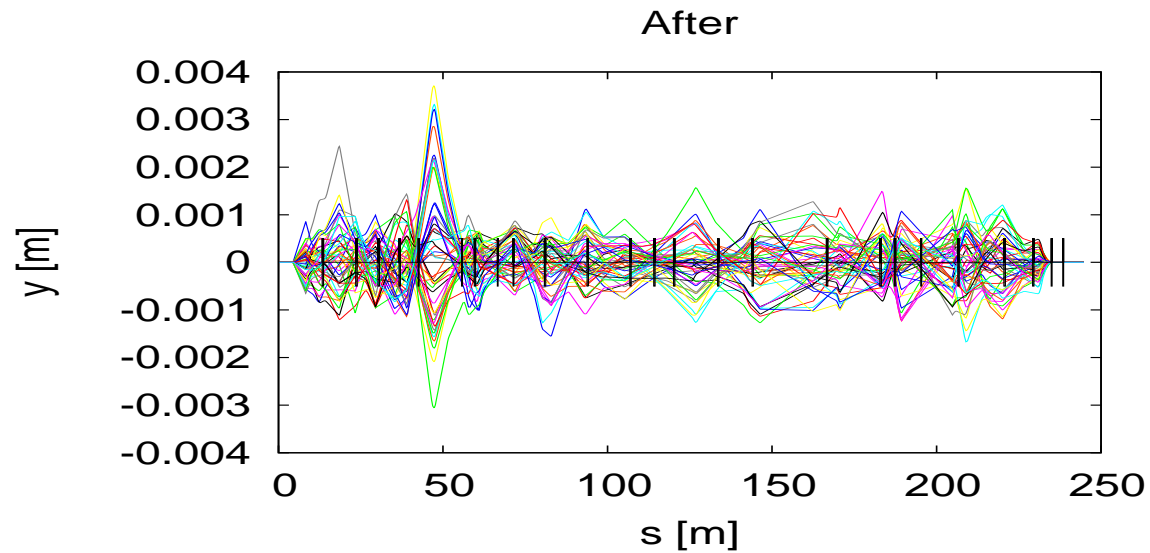
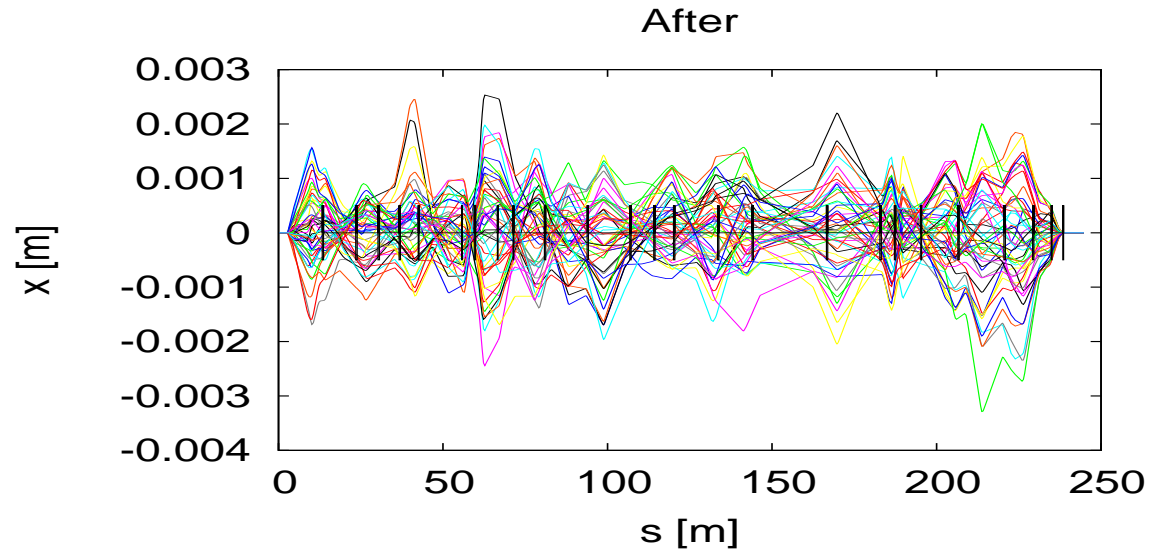
x_{rms}	\hat{x}	y_{rms}	\hat{y}
0.736 ± 0.519	2.395 ± 1.749	0.380 ± 0.161	1.432 ± 0.831

Maximum correction kick (mrad)(*)

$\langle \hat{\theta}_x \rangle$	$\langle \hat{\theta}_y \rangle$
0.324 ± 0.188	0.316 ± 0.102

(*) Averages over 50 seeds quads misalignment and 10% monitor calibration error

500 μm monitor rms offset (50 seeds)



500 μm monitor rms offset (*cont.*)

After correction (mm)(*)

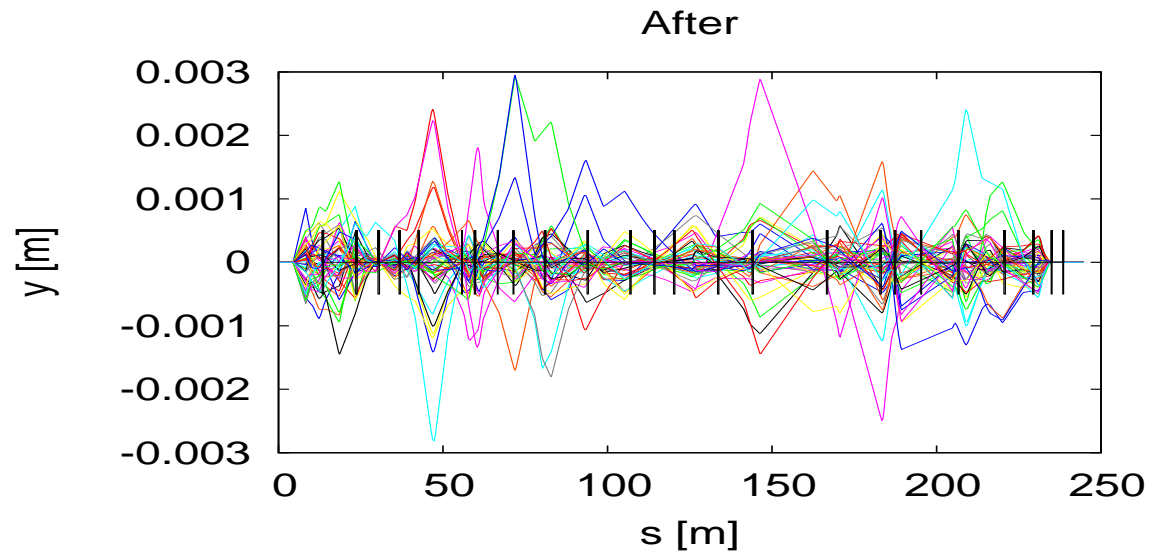
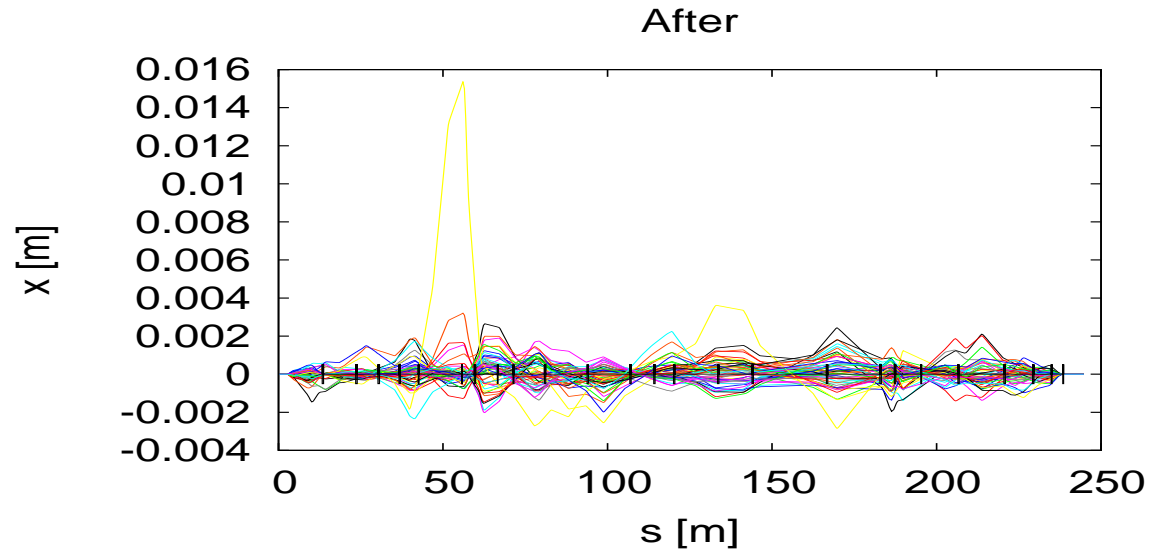
x_{rms}	\hat{x}	y_{rms}	\hat{y}
0.569 ± 0.126	1.677 ± 0.456	0.498 ± 0.109	1.992 ± 0.737

Maximum correction kick (mrad)(*)

$\langle \hat{\theta}_x \rangle$	$\langle \hat{\theta}_y \rangle$
0.287 ± 0.134	0.381 ± 0.115

(*) Averages over 50 seeds quads and monitors misalignment

80% monitor availability (50 seeds)



80% monitor availability (*cont.*)

After correction (mm)(*)

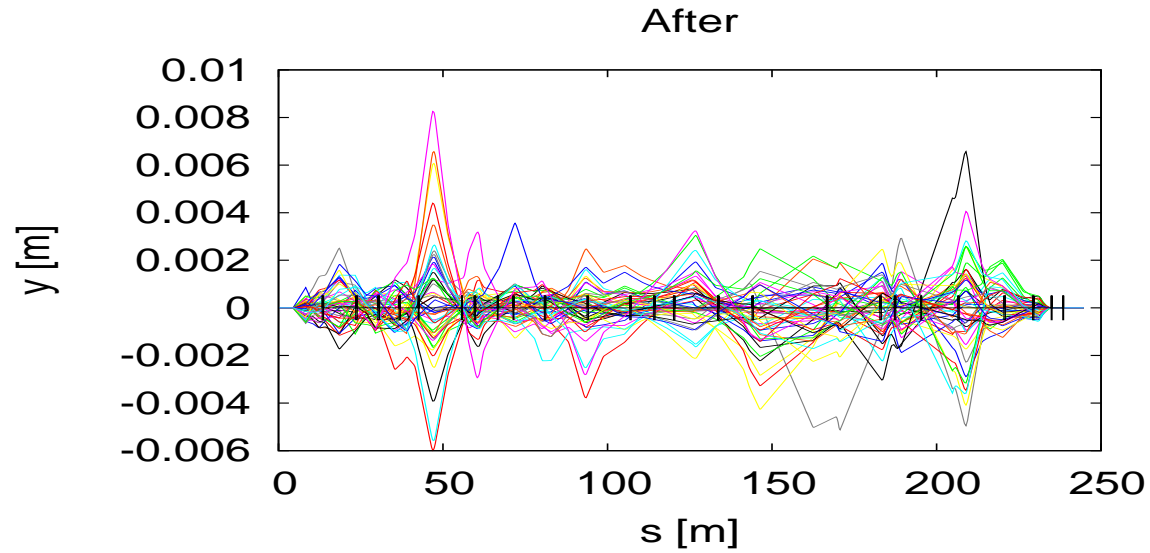
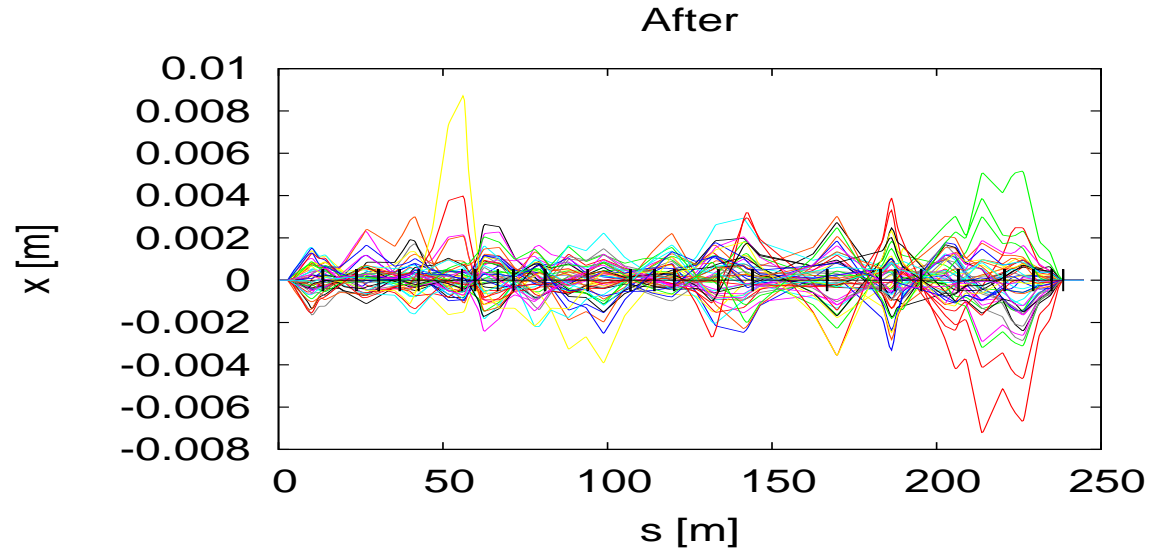
x_{rms}	\hat{x}	y_{rms}	\hat{y}
0.506 ± 0.423	1.729 ± 2.029	0.310 ± 0.126	1.289 ± 0.693

Maximum correction kick (mrad)(*)

$\langle \hat{\theta}_x \rangle$	$\langle \hat{\theta}_y \rangle$
0.318 ± 0.245	0.277 ± 0.086

(*) Averages over 50 seeds quads and monitors misalignment

10% monitor calibration error + 500 μm monitor rms offset + 80% availability
(50 seeds)



10% monitor calibration error + 500 μm monitor rms offset + 80% availability (*cont.*)

Averages over 50 seeds

	x_{rms} (mm)	\hat{x} (mm)	y_{rms} (mm)	\hat{y} (mm)
before	4.854 ± 2.392	15.193 ± 8.323	3.877 ± 1.687	12.593 ± 6.303
after	0.811 ± 0.368	2.558 ± 1.428	0.912 ± 0.552	3.934 ± 3.873

Maximum correction kick (mrad)

$\langle \hat{\theta}_x \rangle$	$\langle \hat{\theta}_y \rangle$
0.341 ± 0.173	0.479 ± 0.284

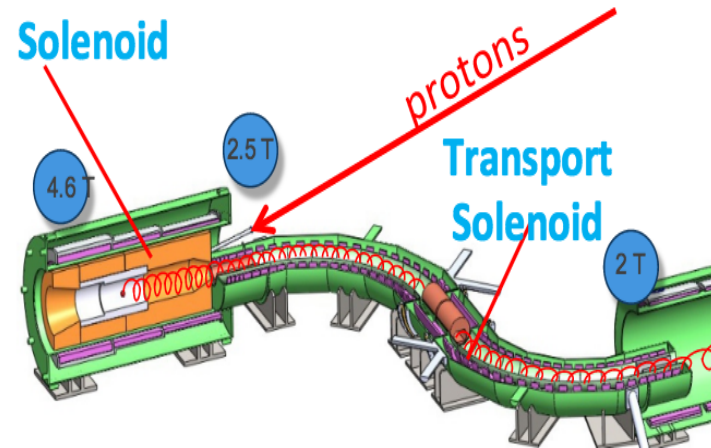
Outlooks

Next steps

- Account for actual gradient seen by the extracted beam at the DR quadrupoles.

- Include production solenoid field.

- ???



Extra slides

MADX Survey

M4 magnet survey and optics are computed by MAD-X.

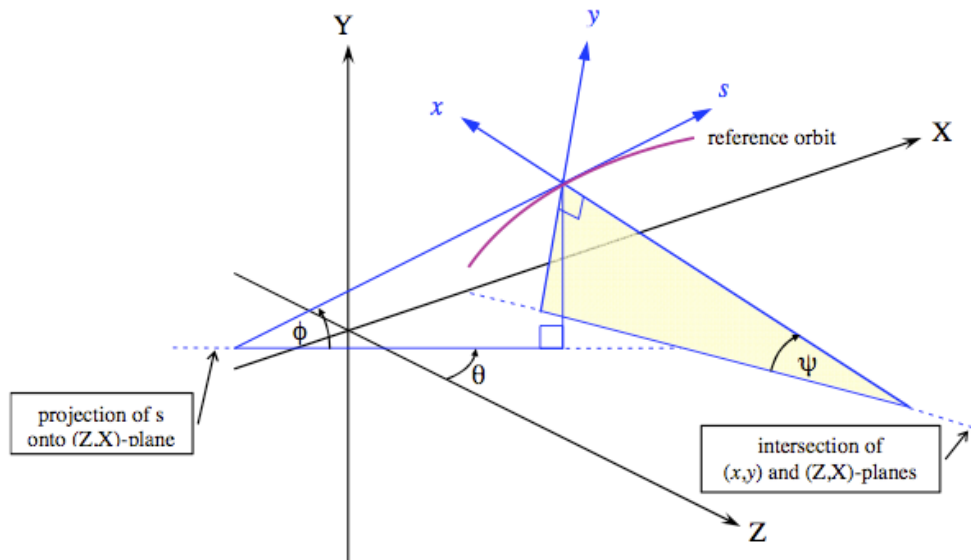


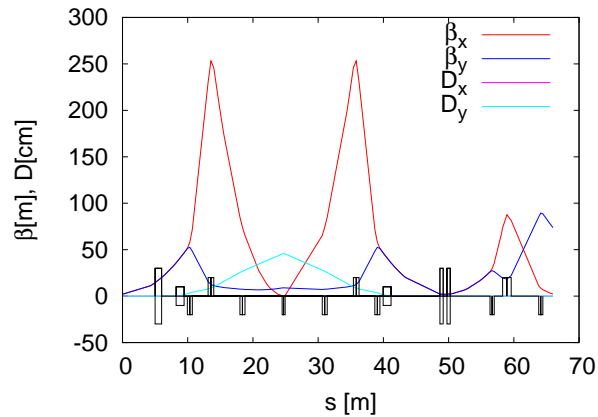
Figure 1: Mad Reference System

ψ becomes non-zero when a *horizontal* bending magnet at $\phi \neq 0$ is encountered (torsion). The code assumes that the following magnets are rolled around \hat{s} accordingly.

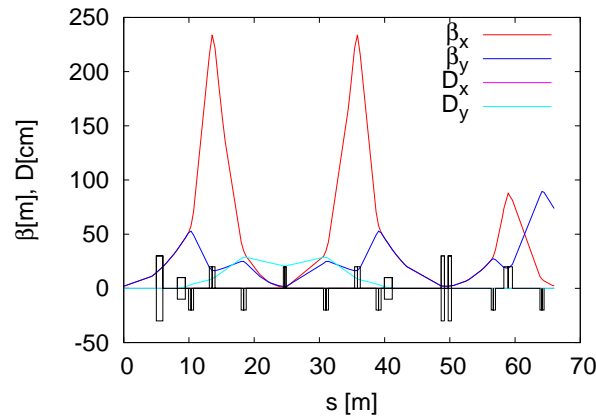
For technical reasons the first M4 dipole is only *almost* vertical (0.6 degrees roll). A rotation of the local frame by -0.0028 degrees must be introduced in the beamline description right after the ECMAG for correctly specifying the actual magnets orientation in the fixed frame.

Polarity flip

The polarity flip does not preserve the dispersion. It is possible to re-match the FF for canceling the vertical dispersion:



middle quad on



middle quad off

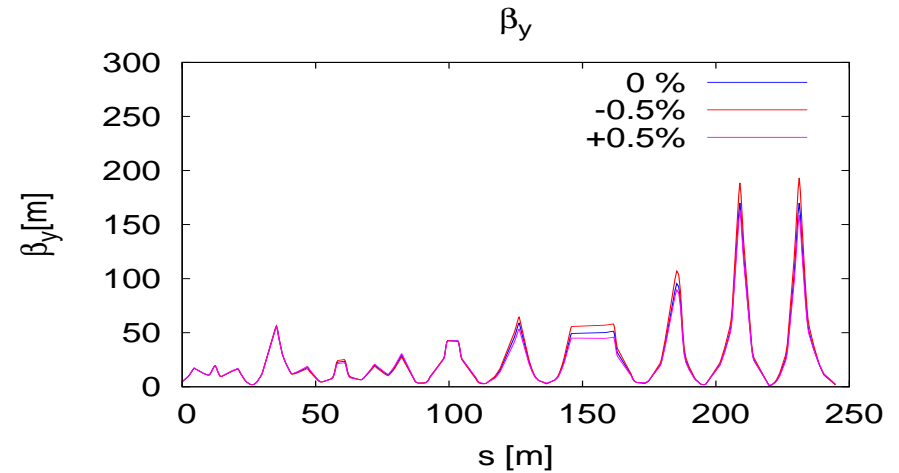
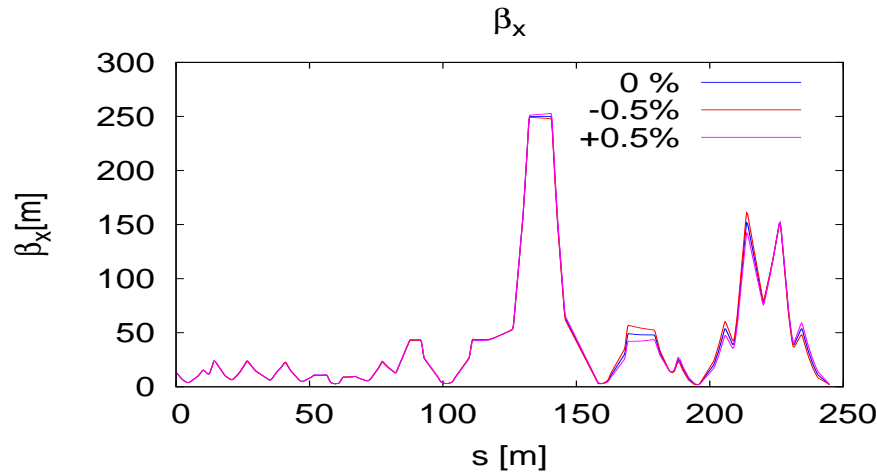
These FF optics have a larger $\hat{\beta}_x$ but smaller $\hat{\beta}_y$; however they are *not* more convenient than the inverted polarity optics for the vertical angle scans.

Off-energy optics

The momentum dependence of the optics seems to be so far acceptable.

It may be improved *if needed* by decreasing the strength of some quadrupoles.

A possible alternative



	quads	p.s.	$\langle \beta_x K \ell \rangle$	$\langle \beta_y K \ell \rangle$
baseline	43	33	3.1	2.9
"alternative"	52	40	2.8	2.9